ade 950 313

AD A122256

TECHNICAL REPORT RE-81-27

A DISPERSED RADAR CONCEPT FOR AIR DEFENSE

William G. Spaulding

Advanced Sensors Directorate,
US Army Missile Laboratory

July 1981

U.S. ARMY MISSILE COMMAND
Redstone Arsenal, Alabama 35809

DTIC
ELECTE
DEC 10 1982

D

82 12 08 013

DISPOSITION INSTRUCTIONS

DISCLAIMER

TRADE NAMES

SECURITY CLASSIFICATION OF THIS PAGE (When Data Entered)

REPORT DOCUMENTATION PAGE		READ INSTRUCTIONS BEFORE COMPLETING FORM
1. REPORT NUMBER RE-81-27	2. GOVT ACCESSION NO. AD A122 256	3. RECIPIENT'S CATALOG NUMBER
4. TITLE (and Subtitle) A Dispersed Radar Concept for Air Defense		5. TYPE OF REPORT & PERIOD COVERED Technical
		6. PERFORMING ORG. REPORT NUMBER
7. AUTHOR(s) William G. Spaulding		8. CONTRACT OR GRANT NUMBER(s)
9. PERFORMING ORGANIZATION NAME AND ADDRESS Commander US Army Missile Command ATTN: DRSMI-RE, Redstone Arsenal, AL 35898		10. PROGRAM ELEMENT, PROJECT, TASK AREA & WORK UNIT NUMBERS
11. CONTROLLING OFFICE NAME AND ADDRESS Commander US Army Missile Command ATTN: DRSMI-RPT, Redstone Arsenal, AL 35898		12. REPORT DATE July 81
		13. NUMBER OF PAGES 55
14. MONITORING AGENCY NAME & ADDRESS(if different from Controlling Office)		15. SECURITY CLASS. (of this report) UNCLASSIFIED
		15a. DECLASSIFICATION/DOWNGRADING SCHEDULE

16. DISTRIBUTION STATEMENT (of this Report)

Approved for public release; distribution unlimited

17. DISTRIBUTION STATEMENT (of the abstract entered in Block 20, if different from Report)

18. SUPPLEMENTARY NOTES

19. KEY WORDS (Continue on reverse side if necessary and identify by block number)

Radar   Bistatic
Antenna   Array
Digital Beamforming   Surveillance Radar

20. ABSTRACT (Continue on reverse side if necessary and identify by block number)

This paper suggests a radar configuration for long range (200 km), air defense surveillance. The configuration proposed is multi-static; e.g., several transmitters are used to host one or more receivers. The transmitters are located within a region, or "farm", of a few hundred meters in extent which is displaced from the receiver by several hundred meters. By spatially distributing the transmit function in this fashion, and displacing it from the receive site, the transmit units can be blinked in a manner similar to that of decoys deployed for

monostatic radars. In the approach proposed here, the radiation from the "decoys" is used as the actual radar transmitter.

The report discusses illumination, waveforms, and multiple beamforming trade-offs necessary to perform efficient radar operation. It further suggests development efforts which must be conducted before such a system is ready for operational use.

CONTENTS

A DISPERSED RADAR CONCEPT FOR AIR DEFENSE

I. INTRODUCTION

This paper suggests a radar configuration for long range (200 km), air defense surveillance and acquisition*. The configuration proposed is multi-static; e.g., several transmitters are used to host one or more receivers. The transmitters are located within a region, or "farm," of a few hundred meters in extent which is displaced from the receiver by several hundred meters. By spatially distributing the transmit function in this fashion, and displacing it from the receive site, the transmit units can be blinked in a manner similiar to that of decoys deployed for monostatic radars. In the approach proposed here, the radiation from the "decoys" is used as the actual radar transmitter.

Figure 1 indicates a typical equipment layout as described above. Three transmitters are shown as hosts to one receive site. The distances shown are typical of those required to separate the transmitters from the receive site in order to prevent ARM impact at the receive site. Separation shown between transmit sites is typical of that used for decoy farm distribution.

It will be noted that transmit and receive separation is small compared to the detection range of the radar. This has the advantage that the target range and doppler determination is not very sensitive to the multi-static geometry, compared to widely dispersed multi-static systems. Secondly, the useable coverage air space is similar to that of monostatic radar; and thirdly, the equipment interfaces and logistics are greatly simplified by these short distances. On the other hand, one of the primary advantages of widely dispersed multi-static radar is not obtained here, that of reducing the distributed clutter size for range ambiguous systems.

---

*There appears to be some confusion in the radar community over the classification of surveillance, acquisition, or search functions as associated with a particular type of radar. The Navy seems to "search" for long range targets; whereas, the Army "surveys" the combat zone or "acquires" targets for weapon engagement. Historically, the terms were reputed to belong to one development command or another with mission connotation somehow involved. The terms will be considered vaguely synonymous for the purposes here. The radar described is intended to detect and track aircraft targets in a tactical air space environment in the presence of electronic countermeasures and hostile anti-radiation missiles.
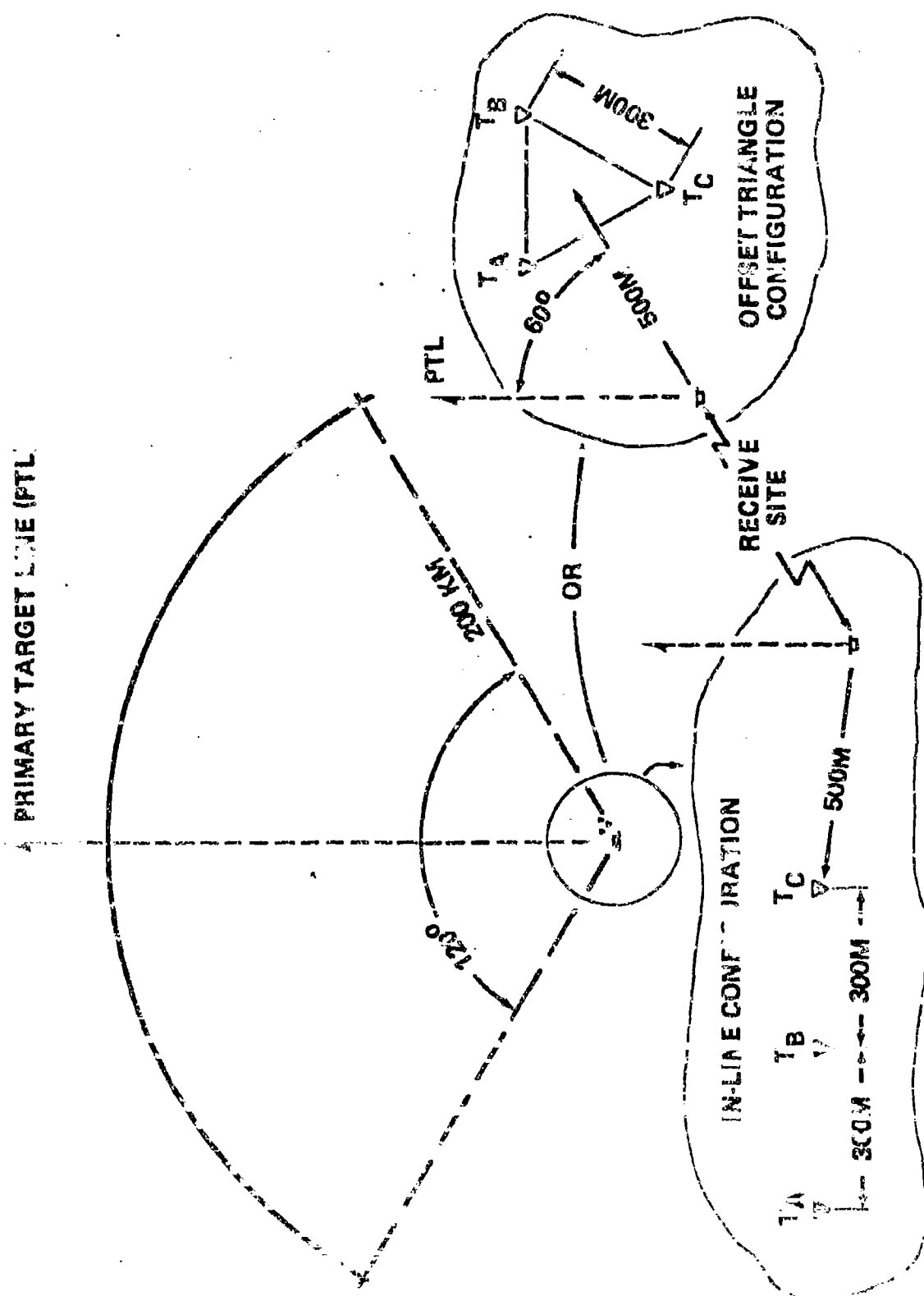
Figure 1. Typical equipment layout for the dispersed radar

II. Configuration Rationale

A. Air Defense Surveillance Role

Tactical air defense systems for high altitude, long range targets need surveillance radar functions in order to (1) assess a raid threat as it develops; (2) prioritize raid sectors, primary target lines, and target groups; and (3) enable the battery or division commander to assign and designate targets to defense units. As the battle develops the surveillance radar is needed for kill assessment and re-direction of force to concentrated or breakthrough areas of surviving aircraft.

Both PATRIOT and HAWK have long range surveillance capability. The PATRIOT's fire unit autonomously performs its own surveillance, acquiring and tracking scores of targets simultaneously for assessment and possible engagement. This requires that each PATRIOT fire unit radiate on a continuous basis; each becomes a high value, prime target for an anti-radiation missile (ARM) or electronic intelligence (ELINT) precision location equipment. These concerns produce significant costs to the system in terms of ARM decoys and fast march order and emplacement times for frequent re-positioning of equipment.

The Hawk pulse acquisition radar (PAR) and the improved CW acquisition radar (ICWAR) are designed to provide target acquisition for the HAWK battery. The HAWK radars and missile launchers are dispersed; but the long range radars are still prime targets for ARM and ELINT suppression and identification.

Autonomous surveillance capability at the fire unit or battery command level is (and will always be) necessary and vital. There is significant advantage to the battery commander; however, if this surveillance capability is augmented with an independent equipment for that special purpose: (1) The weapon radars do not need to radiate prior to the battle, and their high power, long range search waveforms can be cut back or eliminated during an ARM attack. (2) Decoy farms can possibly be replaced by emission management. (3) During engagement, the weapon radars can be totally dedicated to the engagement and guidance waveforms, with no degradation of surveillance capability due to the need to time share the radar resources.

B. Radar Design for Survivability

Critics of the need for a separate long range surveillance radar for air defense are quick to point out that the high power radar, on a fixed site, would provide good ARM fodder for the first day of the war. After that, the fire units would be on their own anyway -- and thus the need for only autonomous capability. This criticism accurately points to the fact that the surveillance radar must be designed to survive and operate effectively in an ARM and ECM environment. If this were not the case, there are any number of air traffic control radars that could be militarized to fulfill this role.

This survival premise must be a basic consideration for new military radar design. Thus far, techniques to counter the ARM threat fall into two general categories: (1) Those used for new radar design specifically addressing the ARM problem, and (2) those used as "band aid" fixes on existing radars. A discussion of these two classes follows for the long range application.

1. New "ARM proof" design...The average power radiated by a 200 km radar is too high to hide with signature control. Quiet or low probability of intercept waveforms, coupled with frequency agility serve to reduce the number of discriminants available to the ARM, but even with ultra-low sidelobe antennas, there is adequate sidelobe radiation for ARM homing from ranges well beyond the detection range of the radar. The 200 km radar requires more than signature control; although the low peak power waveforms certainly are a step in the right direction.

2. "Band aid" fixes...These are applied to radars already fielded and generally take the form of either emission control measures or decoys. Emission control requires "blinking," or cycling the radar transmission on and off with the time of the off periods roughly a factor of two to three times that of the on periods. If full time coverage is required, the radar must be netted to others with similar air space coverage to allow the radiation on-time to be alternated between radars. Obviously, if autonomous operation is required, the blinking will significantly degrade the data rate of the single radar.

If decoys are chosen as the ARM countermeasure, they must be powerful enough to equal or exceed the sidelobe radiation of the radar. For radars of this class and vintage this means that the decoys must be almost as powerful as the radar transmitter. For example, if we assume the radiated power from the decoy must at least equal the radiated sidelobe power of the radar, we have

$$P_t G_{sl} = P_d G_d$$

where P_t is the radar transmitter power, G_{sl} is the gain of the radar sidelobes, P_d is the decoy transmit power, and G_d is the gain of the decoy antenna. The gain of the peak sidelobes for typical radar antennas of interest ranges from about 2 to 10 dBi. If the gain of the decoy antenna is equal to this gain of the sidelobe of the radar, the decoy power must also equal the radar transmit power. If the decoy antenna gain is increased beyond 5 dB, the coverage of the decoy is reduced from hemispheric coverage as shown by Figure 2. For example, if a decoy is designed to cover a 10 dBi sidelobe, and if its transmitter power is one half of (3 dB less than) the radar transmitter power, its antenna gain must be 13 dB; therefore, from Figure 2 the single decoy would only cover a sector that is 45 degrees in azimuth by 60 degrees in elevation. If a 90° Az by 60° El sector is to be covered, a second decoy this size must be added, or a decoy transmitter of the same power as the radar. The point is that decoying a 200 km radar requires a significant equipment expenditure.

A more effective solution to the ARM problem is to separate the transmit site from the receiver using a bistatic or multi-static geometry. Thus,
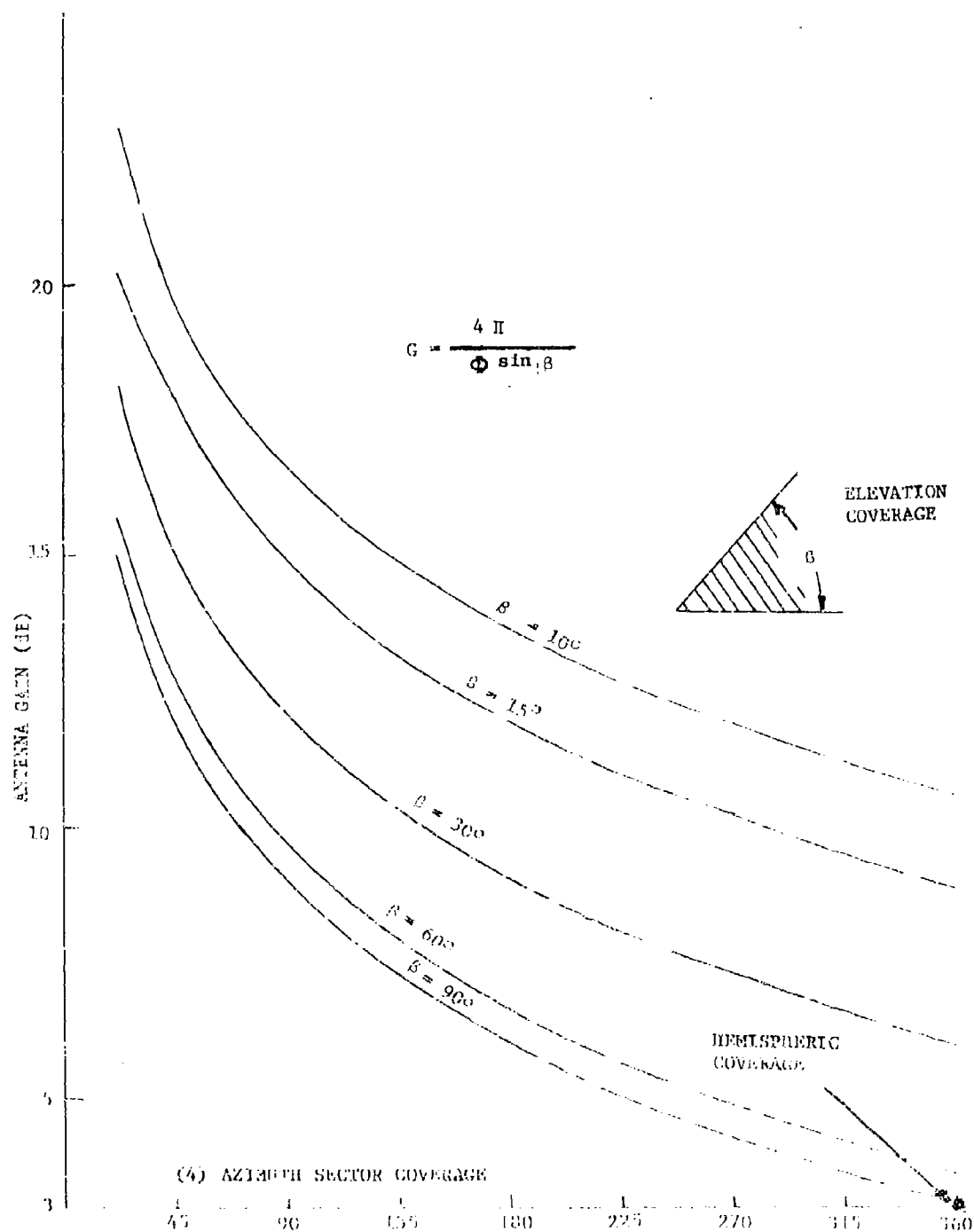
Figure 2. Available array antenna directive gain versus antenna coverage

the receive site can stay quiet, away from the radiation signature, and immune from the ARM. To protect the transmitter, previous concepts have placed it far from the FEBA and out of reach by the ARM. Generally, this requires an airborne transmitter. The configuration proposed here is of the multistatic class; however, the remote, airborne site is not necessary.

C.   Radar Design for Reduced Susceptibility to ECM

In addition to surviving the hard kill of the ARM, the radar performance must also survive the soft kill of ECM. Modern jamming threats require the use of a pencil beam to reduce the extent of the main beam susceptibility to being jammed. Secondly, the lowest side lobe levels affordable are needed to reduce the effect of sidelobe jamming from stand-off jamming. Adaptive measures of several classes are being investigated by the radar community to further reduce jamming effects. Most of these involve reducing the sensitivity of the antenna pattern in a selective manner to the specific direction of the jammer. Techniques for both closed loop and open loop adaption are under investigation for this purpose. The success of these techniques depends on the number of degrees of freedom available to establish an illumination function for the antenna (which produces the required nulls in its spatial response) and the speed at which this can be accomplished. The proposed configuration offers the possibility of evolutionary growth in this area since the response of each element of the receive array is available to the processor.

D.   Advantages for the Multistatic Configuration Proposed

In order to counter the hostile environment outlined above, the radar proposed here is quasi-multistatic (or quasi-monostatic); e.g., the transmitter is separated from the receiver, but not very far. The transmit-receiver baseline is roughly .003 times the detection range. In addition, the transmitter is spatially distributed. This means that the average power required to detect aircraft at 200 km is derived from perhaps a total of three units rather than a single transmitter. This reduces a given transmitter size and allows them to be separated from each other by several hundred meters as shown in Figure 1. Modest separation of the transmit and receive functions provides enough isolation to reduce the requirements of the TR device for a pulsed radar. It should allow the use of flexible coded CW waveforms. It should also reduce the return from near-in clutter. More significantly, this separation allows protection of the high value passive receive site and its personnel from ARM attack or precise ELINT location. Suppression of power will be brought to the transmitter from a safe distance away from the receive site. Furthermore, the antenna complexity is somewhat offset by this separation, since the more sophisticated requirements of beam formation, etc., are placed on the receive function only. The transmit (high power) antenna is a relatively simple, low microwave loss device.

When compared to other multistatic radar concepts which use single airborne transmitters in a remote location, there are distinct advantages. All equipments are on a fixed site. Once located, dynamic compensation is not necessary in the multi-static location equations. The clutter is not complicated by doppler due to the transmit platform movement. Near co-location

6

(compared to widely dispersed systems) gives fewer calibration and control problems. It also implies that the total transmit power requirement is similar to that of the monostatic radar. Since the transmit and receive functions are not widely dispersed, the masking is similar to that of a monostatic radar; therefore, extreme elevation of the transmitter is not necessary. The distributed transmitter can be organized to reduce its vulnerability to ARM's through blinking, frequency diversity, antenna sector switching, etc. A direct hit on one transmitter may reduce the detection range of the system but "graceful degradation" occurs with transmitter attrition. Each transmitter is a fairly simple device and does not have to provide the entire radiated power of the radar.

III. Coverage

A. Tradeoffs

Given the need for a multistatic system, there are a number of choices in its configuration. The use of a distributed transmitter limits these choices. Because of the number of transmitters employed here, their design must be simple. Pencil beam transmitters synchronized with pencil beam reception do not meet this criterion. Rotating transmit fan beams require less synchronization with the receiver; however, the data stream and dwell time budget are confined by the rotation rate. At the opposite extreme, omni-directional transmit beams waste too much coverage-power product since a multiple beam receiver covering the same hemisphere of space is impractical. Most of the idealized multistatic configurations are not practical for long range radar applications simply because of the inefficiency encountered when one tries to register, or overlap, the transmit coverage with the receive coverage.

B. Proposed Approach

The approach chosen uses a sector coverage transmit beam that is matched to the coverage of a cluster of receive pencil beams. Both the transmit and the parallel receive beams are fixed spatially for a detection dwell period. Then the transmit beam and the entire receive beam cluster are moved simultaneously to interrogate another sector. During a given sector dwell period, the transmit beam may be derived from one or perhaps all of the transmitters in the farm in a sequential fashion. The transmit scheme will depend on the dwell time required by that sector, and may be altered subject to ARM attack or equipment condition.

Since the receive beam cluster is scanned as a group, special attention must be given to a tracking scheme for high priority targets. In order to provide a more precise target location for track, it may be necessary to provide elevation and azimuth difference beams which are scanned independently from the receive beam cluster. This can be accomplished through extension of the digital beam forming processor with no RF hardware changes. It should be noted, however, that the data rate is still paced by the step scan of the transmit flood beam among the minor sectors. If a higher data rate is required, it could be supported by extra illumination of the track sector, using one of the

7

transmitters out of the normal sequence used for search coverage. Tracking details will not be further addressed here.

This concept could be implemented over a 360 degree azimuth region using antennas which employ the dome lens techniques; however, a major sector coverage of 120 degrees in azimuth is suggested here because (a) most long range air defense scenarios have primary interest in the air space over the FEBA and beyond; and (b) sector coverage allows the use of planar arrays, which are technically staight forward and serve to illustrate this example system. However, it should be noted that the multiple beam receive system inherently provides very fast data rates (to be shown later herein). This indicates that the frame time limitations generally associated with sequentially scanned pencil beams over large regions of air space are relaxed; therefore, growth of this construct configuration to hemispheric coverage is feasible. The risk to this growth is primarily one of added complexity and cost rather than technical, given the achievement of the sector coverage system. This is based on the results of the Hemispheric Coverage Antenna work at Sperry in the US. Hardware was built and evaluated, showing that a pencil beam, with good integrity, can be scanned over a hemisphere from a planary array feeding a dome shape microwave lens.

C. Sector Allocation

The 120 degree azimuth sector of Figure 1 is divided into nine minor sectors. These are shown on the orthographic projection of Figure 3. The nine are stacked, three in azimuth by three in elevation. The elevation coverage profiles are shown on the altitude versus slant range chart of Figure 4. These sector sizes were chosen to accommodate about 200 receive (2 degree) pencil beams each. The number, 200, is not optimized. It was selected as a reasonable goal for the number of simultaneous beams to be digitally formed and processed in real time with the advent of Very High Speed Integrated Circuits (VHSIC) expected in the 1990's.

D. Receive Beam Requirements

The receive site uses a single planar array, fixed in position, with its broadside beam oriented in azimuth toward the primary target line (PTL). It is tilted back in elevation in order to minimize the encroachment of grating lobes for the scan volume to be covered. This also minimizes the number of elements required in the array. The tilt back angle is determined in Appendix A as 13.1 degrees from the vertical.

In order to examine coverage in detail, the usual array coordinates are defined in Figure 5 where α and β are scan angles in orthogonal planes intersecting in a line which is normal to the center of the array plane. These angles are related to earth coordinates azimuth, Az, and elevation, El, when the array is tilted back from the vertical by the angle T, as follows*:

* Figures 2 and 5 are considerably more on the coordinate systems and their interrelationships.

ARRAY NORMAL
13.1° TILT

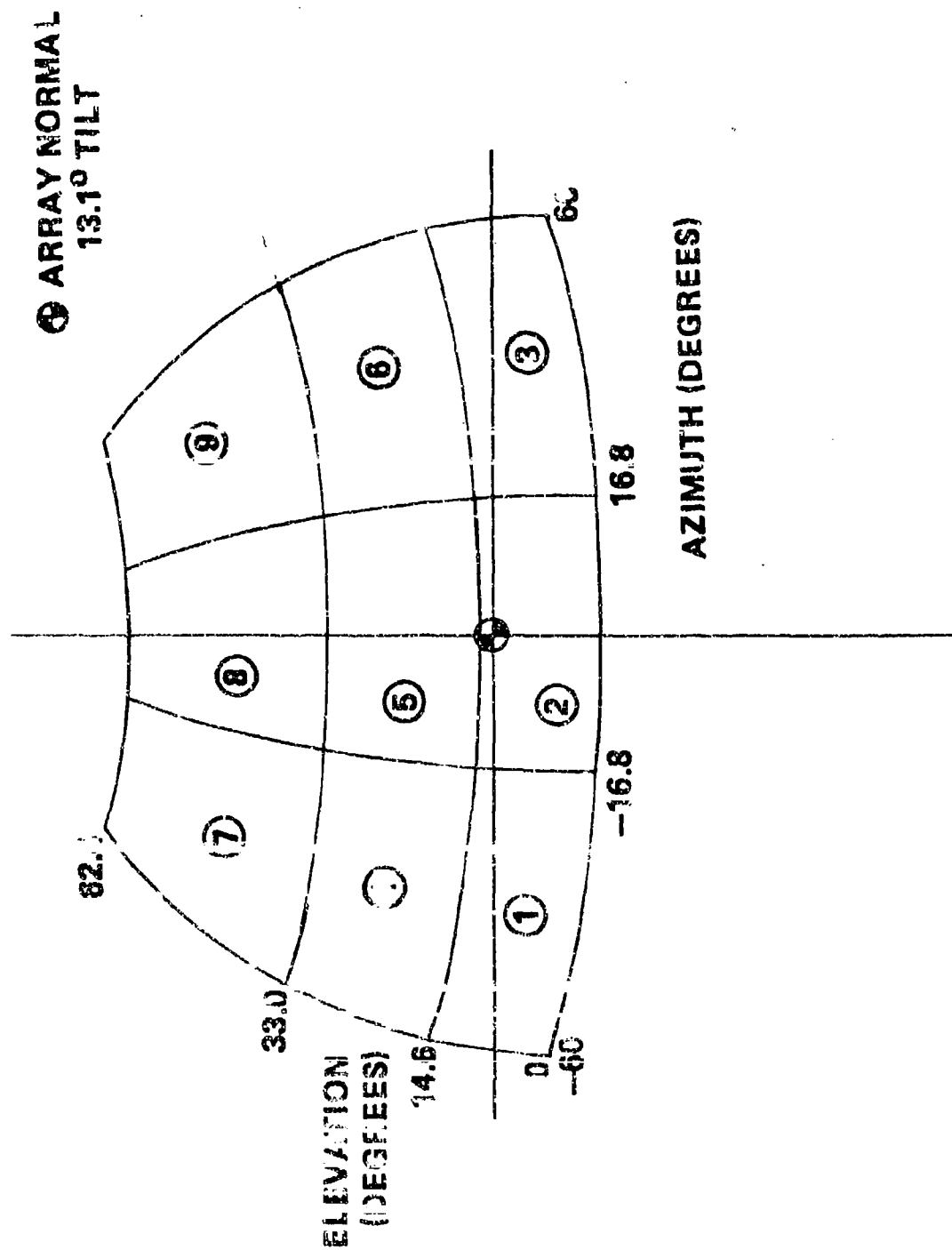AZIMUTH (DEGREES)

16.8

−16.8

60

ELEVATION
(DEGREES)

82.3

33.0

14.6

0

−60

Figure 3. Orthographic projection of example coverage sectors
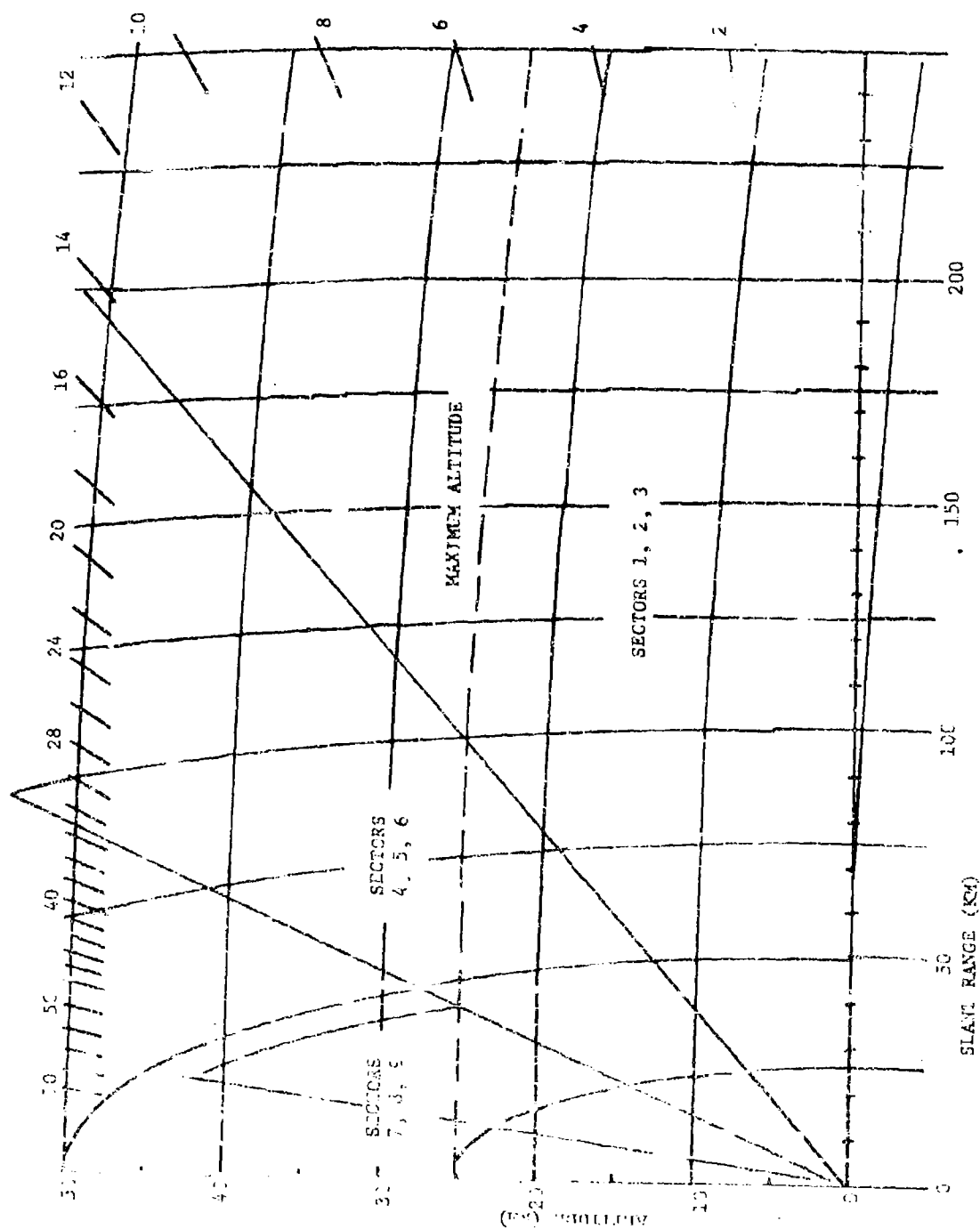
Figure 4. Elevation coverage of stacked sectors

X, Y — plane of the array

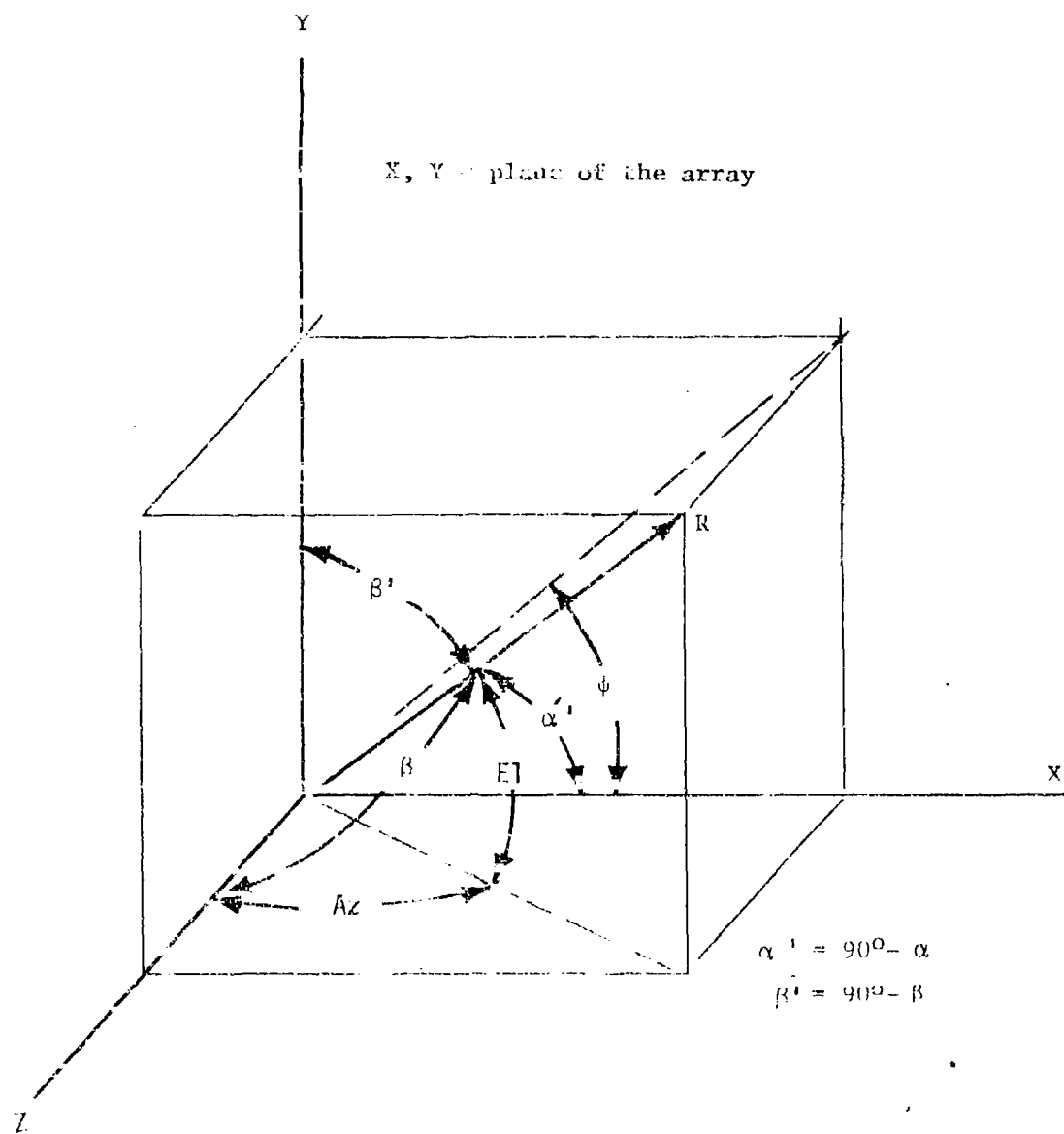$\alpha^{1} = 90^{0} - \alpha$

$\beta^{1} = 90^{0} - \beta$

Figure 3. — Spherical and array coordinates. Az and El shown for no tilt.

$$\sin \alpha = \cos El \sin Az \qquad \qquad (III-1)$$

$$\sin \beta = \cos El \cos T - \cos El \cos Az \sin T \qquad (III-2)$$

The beamwidth of an array that is fixed in space broadens as it is scanned from broadside by $1/\cos \theta$ where θ is the angle from broadside to the scan direction. However, when the beam is projected to the $\sin \alpha$, $\sin \beta$ coordinate plane, its dimensions are invariant with scan. Therefore, adjustment of coverage of space with a number of sequentially scanned beams (or parallel simultaneous beams) is usually done in "sine space." The 2 degree beamwidth of this example translates to 35 millisines. This 35 millisines can be used for the beamwidth over all of the scan space.

If the ensemble of simultaneous receive beams must cover a given transmit sector, their scan directions must be chosen using a rationale which involves a trade off between the number of beams required and the average loss of gain over the sector coverage. For example, Figure 6 indicates three ways of stacking the receive beams, where the circles shown represent the 3 dB contour of the beam in sine space.

For this example, the receive beams will be stacked as in Figure 6-C. This is chosen because it provides the lowest loss; hence, a reduction in transmitter power requirements. By applying this stack lattice of .75 beamwidths x .866 beamwidths to $\sin \alpha$, $\sin \beta$ space, the number of beams for a given sector of sine space is easily obtained. This is not very useful; however, because the coordinates of interest are earth coordinates, Az and El, related to $\sin \alpha$, $\sin \beta$ by Equations (III-1, 2). Therefore, the procedure must be reversed, choosing earth coordinate sectors and iterating their limits until each has the number of beams equal to the number of available parallel receivers (in this case, 200). Here, the major azimuth scan region from $Az=-60^{\circ}$ to $Az = +60^{\circ}$ was divided into three regions which have equal extent in $\sin \beta$ space.

(a) from $Az = -60^{\circ}$ to $Az = -16.8^{\circ}$

(b) from $Az = -16.8^{\circ}$ to $Az = +16.8^{\circ}$

(c) from $Az = +16.8^{\circ}$ to $Az = +60^{\circ}$.

From equation (III-1) it can be shown that a row of beams along a given elevation scan (El = constant) will have the same number of beams in each of the above scan regions. Thus, the three sectors which are bounded by these Azimuth limits and constant elevation limits have equal numbers of beams in each. By simple iteration of the lattices of Figure 6-C in sine space, the nine sectors of Figure 3 can be shown to have about 200 beams in each sector when the array is tilted back at 15.1°.

The solid angle, Ω_R, of a single receive pencil beam is given by

$$\Omega_R = 2\pi (1-\cos \delta) \qquad \qquad (III-3)$$
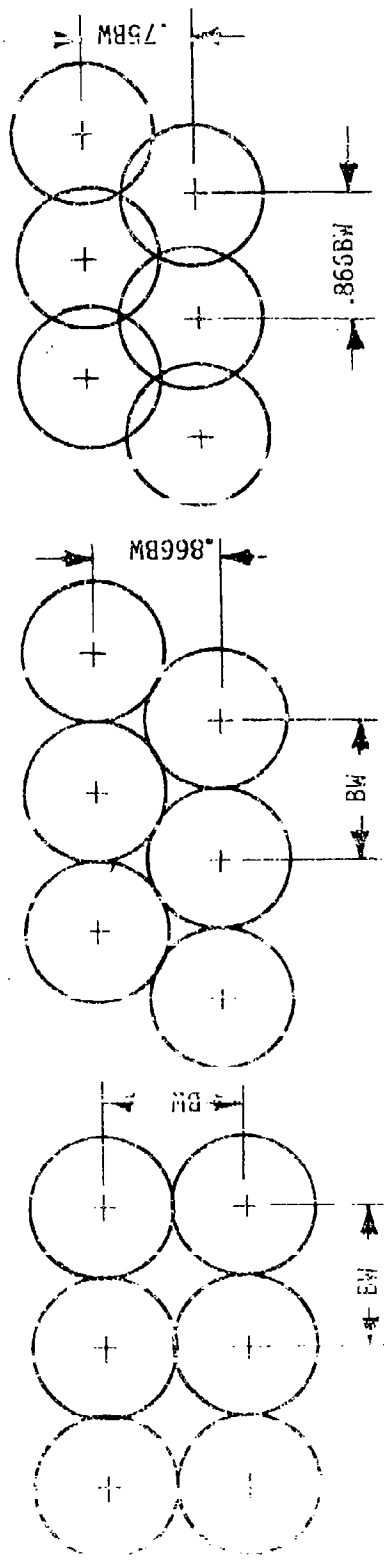
	BW^2	$.866BW^2$	$.650\ BW^2$
Solid Angle per cell			
Number of Beams	N_b	$1.15\ N_b$	$1.54\ N_b$
Average Loss (dB/BW)	$1.7\ dB$	$1.55\ dB$	$1.16\ dB$
	A-Columned Beams	B-Interlaced Beams	C-Low Loss Lattice

Figure 6. Methods for stacking pencil beams in space

where δ is the 3 dB beamwidth. Its directive gain Gr, (uniform illumination and no losses) is

$$G_r = \frac{4\pi}{\Omega_R} \tag{III-4}$$

For a two degree beam, $\Omega_r = 9.57 \times 10^{-4}$ and $G_r = 41.2$ dBi.

A scan loss occurs for each of the receive beams that is displaced from broadside. This is due to the beam broadening already mentioned in connection with the 200 beam coverage sector determination of Figure 3. In order to simplify the time-power computations to follow, an average receive scan loss, L_{RS}, will be computed for each of the minor sectors. As an approximation, this scan loss will be taken as the average of five beam positions, one at each corner of the sector and one in the center. A given beam position scan loss, l_{RS}, is given in dB as

$$l_{RS} = 10 \log\left[\frac{1}{\cos\theta}\right] \tag{III-5}$$

where θ is the angle of scan from broadside,

$$\theta = \cos^{-1}\left(\sin El \sin T + \cos El \cos Az \cos T\right). \tag{III-6}$$

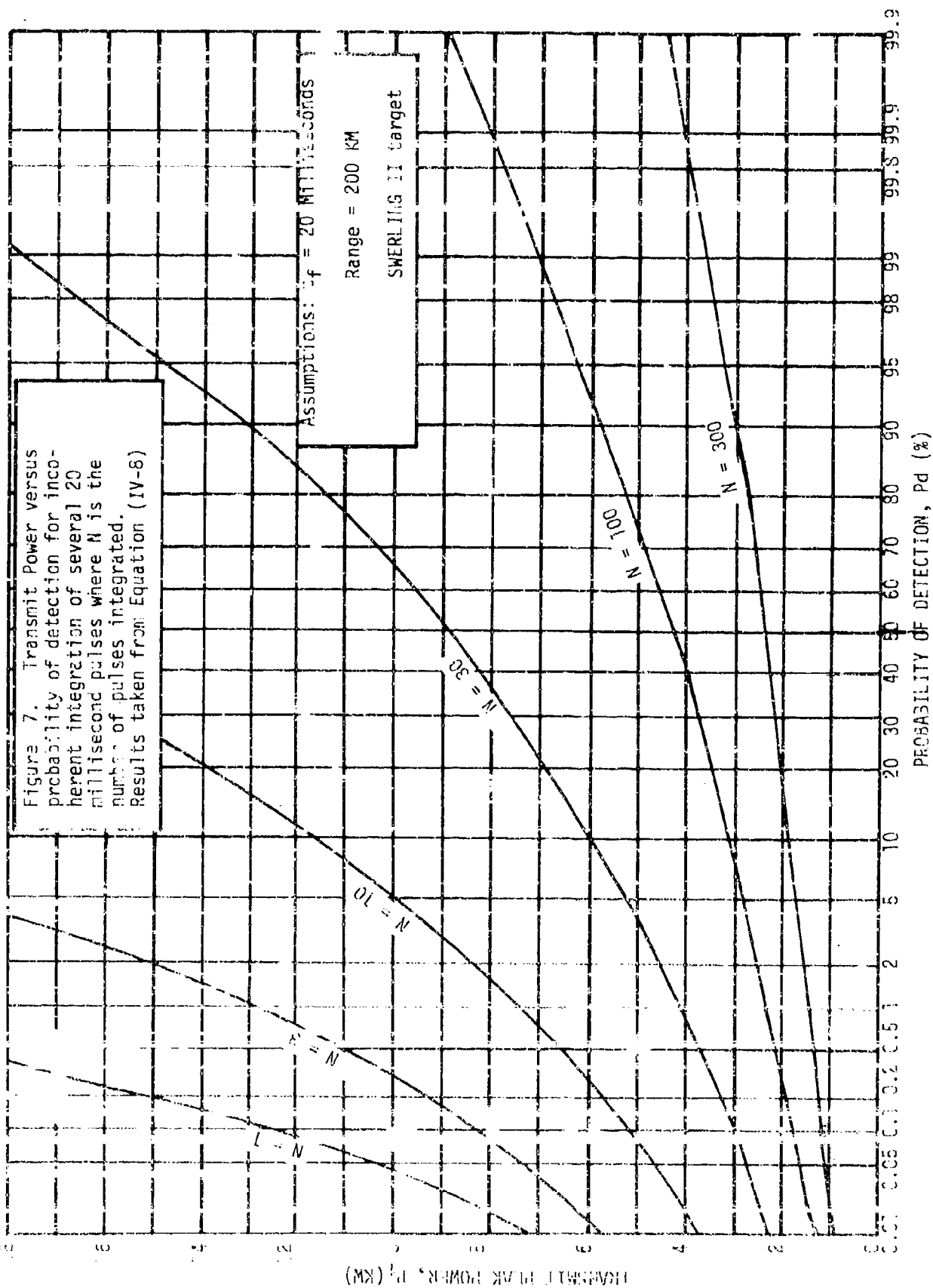The average receive scan loss, computed as above, for each of the minor sectors of Figure 3 is given in Table III-A.

Table III-A. The average scan loss for the receive beams of each of the minor sectors.

SECTOR (see Fig. 7)	L_{RS} (-dB)
1, 3	1.25
2	0.09
4, 6	1.29
5	0.26
7, 9	1.96
8	1.07

E. Transmit Beam Requirements

The minor sectors to be illuminated by the transmit beams are defined by the 2000 beam limits of the receiver as derived above and shown in Figure 7. Each of the dispersed transmitters must be capable of sequentially covering all nine of these minor sectors. In principle, the full transmit power of a given unit can be switched from one sector to another. There is a small amount of overlap between sectors not shown in Figure 3.

Figure 7. Transmit Power versus probability of detection for incoherent integration of several 20 millisecond pulses where N is the number of pulses integrated. Results taken from Equation (IV-8)

Assumptions: τ_f = 20 Milliseconds

Range = 200 KM

SWERLING II target

PROBABILITY OF DETECTION, Pd (%)

TRANSMIT PEAK POWER, P_t (KW)

N = 1
N = 4
N = 10
N = 30
N = 100
N = 300

The solid angle, Ω_t, of a given sector is determined from

$$\Omega_t = \phi_a(\sin El_{max} - \sin El_{min}) \qquad (III\text{-}7)$$

where ϕ_a is the total angular azimuth coverage of the sector in radians, El_{max} is the maximum elevation angle and El_{min} is the minimum elevation angle of the sector coverage.

The directive gain of the transmit beam, G_t, for uniform illumination and no losses, is given by

$$G_t = \frac{4\pi}{\Omega_t} \qquad (III\text{-}8)$$

The solid angle and gain of each of the minor sector transmit beams, calculated from (III-7) and (III-8), is given in Table III-B.

Table III-B. Transmit Beam Parameters.

Sector (See Fig. 3)	X_t (Steradians)	G_t (dBI)
1, 3	0.1899	18.2
2	0.1477	19.3
4, 6	0.2205	17.6
5	0.1715	18.6
7, 9	0.2580	16.9
8	0.2007	18.0

IV. DETECTION CRITERIA

A. Range Equation Assumptions

The bistatic radar range equation is

$$P_t = \frac{(4\pi)^3 R_t^2 R_r^2 KT_o NF(S/N)_o L}{TG_t G_r \lambda^2 \sigma} \qquad (IV\text{-}1)$$

Where:

P_t = peak transmitted power
R_t, R_r = range to the target from transmitter, receiver
G_t, G_r = Antenna gain of transmitter, receiver
KT_o = product of Boltzman constant and temperature
NF = receive noise figure
$(S/N)_o$ = signal to noise ratio at receiver output
L = total system losses
T = single pulse integration time
λ = wavelength
σ = target cross section.

For this multistatic geometry, where the transmitters are close to the receiver, it will be assumed that $R_t = R_r = 200$ KM. Sector Number 2, from Figure 3, will be defined as a reference sector; its antenna parameters will be used in the range equation in order to determine the power required for various dwell periods. Later, these results are extrapolated for other sectors.

B. Probability of False Alarm Rationale

The multiple channel receiver is made possible by spatial beam forming in the digital processor. In addition, it must also process the data in real time for all of the 200 beams. Some redundancy in processing may be required if tracking beams are also implemented. For these reasons, the detection criteria must result in very few false alarms for the heavily burdened processor to deal with.

Thus, a probability of false alarm (P_{fa}) of 10^{-10} is chosen rather than a more conventional value in the 10^{-6} to 10^{-8} range. This choice requires a few more dB signal to noise ratio for a given probability of detection (P_d).

C. Coherent Dwell Interval

The sector flood transmit scheme proposed for this system implies that long integration time will be required for long range detection if the transmit power is to be kept at an acceptable level. This can be done most efficiently by using a waveform which provides the longest practical coherent (or pre-detection) time, and combines multiples of this interval which are further integrated non-coherently. Assuming that doppler processing will be employed, the maximum coherent integration that can be used will depend on how long a maneuvering target will stay in a single doppler filter. This is determined as follows.

The doppler frequency of a target flying at a radial velocity of V_t is

$$f_d = \frac{2V_t}{\lambda} \qquad \text{(IV-2)}$$

If the target undergoes a constant radial acceleration, its velocity change, ΔV_t causes a change in the doppler as

$$\Delta f_d = \frac{2\Delta V_t}{\lambda} \qquad \text{(IV-3)}$$

The acceleration a_t, is a constant given by

$$a_t = \frac{\Delta V_t}{\Delta t} \qquad \text{(IV-4)}$$

over the interval of time, Δt. Substituting then,

$$\Delta f_d = \frac{2a_t \Delta t}{\lambda} \qquad \text{(IV-5)}$$

17

If it is assumed that the integration was initiated when the target was in the center of a doppler filter, its bandwidth, B_f, would need to be twice the expected change in doppler in order to accommodate an increasing or decreasing excursion. From another perspective, if the sign is known, the intergration may not be initiated when the target doppler is centered in the filter, therefore some safety factor is needed, thus a factor of two is chosen). This yields:

$$B_f = 2\Delta f_d = \frac{4a_t\Delta t}{\lambda}$$

$$(IV-6)$$

Furthermore,[5] the integration interval, $t_f = 1/B_f$ can be no greater than Δt. Therefore,

$$t_f < \sqrt{\frac{\lambda}{4a_t}}$$

$$(IV-7)$$

For a target acceleration of 6 g's and λ = 0.1 meter this results in a 20.1 millisecond limit as the maximum coherent integration time that can be used.

D.   Target Model Assumption

For the calculations that follow a 20 millisecond dwell derived in Section C above is considered as a "single pulse" (from a single transmitter). Since each of the 20 millisecond dwells (pulses) can be from different transmitters, the amplitude of each "pulse" in a given sequence is considered to be a statistically independent random variable, with the same Rayleigh probability density funtion. The initial phases of each pulse in the detection sequence are assumed to be independent with uniform probability densities. Therefore, the target is considered Swerling II for this detection scheme.

E.   Transmit Power Calculation

Equation (IV-1) will be used to first examine the transmit power, P_t required to produce a desired signal to noise at the receiver output, $(S/N)_o$, for a single 20 millisecond dwell interval.

	db	db

	db	db
$(4\pi)^3$	33	
$R_t^2 R_{tr}^2 = (200\text{km})^4$	212	
$KT_o = -204$ dBW		-204
NF $= 6$ dB	6	
L $= 13$ dB (Note 1)	13	
T $= .020$ sec.	17	
$G_t = 18.3$ dB (Note 2)		18.3
$G_r = 36.8$ dB (Note 3)		36.8
$\lambda^2 = (10\text{ CM})^2$	20	
$\sigma = 3\text{m}^2$		4.8
	301	263.9

Therefore,

$$P_t = 37.1 + (S/N)_o \qquad\qquad (IV-8)$$

where P_t is in dBW and $(S/N)_o$ is in dB.

NOTE 1: This is an assumed number for the total of the processing and propagation losses.

NOTE 2: The transmit gain of Sector 2 was used here from Table III-B after degrading by one dB to account for feed losses and illumination function inefficiency of the antenna.

NOTE 3: The directive gain of a two degree pencil beam was determined in Section III-D as 41.2 dBi. Ref 3, Table A.17, indicates the efficiency of an n = 8, Circular Taylor illumination function is 0.651 ; therefore, 1.9 dB was subtracted. Feed loss for this antenna was assumed to be 2.4 dB. Table III-A shows a scan loss of .09 dB for this Sector 2. Therefore,

Directive gain	41.2 dB
Illum. Taper	-1.9 dB
Feed loss	-2.4 dB
Scan loss	- .1 dB
G_r =	36.8 dB

The probability of detection, Pd, can now be obtained for the single 20 millisecond dwell interval versus the transmit power. To do this, the $(S/N)_o$ of Equation (IV-8) is replaced by an equivalent Pd which is obtained from the

curves of Chapter 11 of DiFranco and Rubin[2]. These curves indicate the Pd versus peak signal to noise ratio* for various cases of target fluctuation and false alarm parameters. Using the Swerling Case II, N=1, $P_{fa} = 10^{-10}$ curve with Equation (IV-8) yields the N=1 curve of Figure 7 which represents the transmit power required versus Pd for the single 20 millisecond dwell. The DiFranco and Rubin curves for multiple pulses that are incoherently integrated can be applied to multiple units of the 20 millisecond basic dwell. These are shown in Figure 7 for N=1, 3, 10, 30, 100, and 300; where N is the number of these basic dwells that are integrated noncoherently. Figure 7 gives a fairly wide latitude of transmit power levels that could result in, for example, a Pd of 50%. The questions now remain: What data rates result from the choice of P_t? How long can one integrate (noncoherently) for the target detection? These lead to the time-power considerations of the next section.

V. Time-Power Considerations

A. Comparison of Sector Coverage Times

On examination of the Range Equation (IV-1), it is apparent that the dwell time can be expressed in those terms which are likely to have different values from one minor sector of the coverage to the next:

$$T_i = \left(\frac{R^4 Lrs}{G_t}\right) K \tag{V-1}$$

where T_i is the dwell time required in the ith sector for the parameters shown pertaining to that sector. The assumption is made again that $R_r = R_t = R$. Lrs is the average scan loss of the receive antenna as given in Table III-A and G_t is the directive gain of transmit antenna as shown in Table III-B. The rest of the parameters of Equation IV-1 are lumped in the constant, k. Note that the transmit peak power is not varied from sector to sector for practical reasons.

From Figure 4, the approximation will be made that the maximum range to the target for sectors 1, 2, and 3 is twice that in sectors 4, 5, and 6, and four times that of sectors 7, 8, and 9. This occurs because the maximum altitude for targets of interest is 25 km.

The dwell time required by each sector can now be normalized with respect to the reference sector 2:

$$\frac{T_i}{T_2} = \left(\frac{R_i}{R_2}\right)^4 \left(\frac{Lrs_i}{Lrs_2}\right)\left(\frac{G_{t2}}{G_{ti}}\right)$$

---

* FOOTNOTE: The abcissa of these curves is the peak signal to noise ratio in dB, R_ρ, defined as

$$R_\rho = 2A_0^2 \tag{11.2 - 18 of Ref 2}$$

where A_0^2 is effectively the $(S/N)_0$ of Equation (IV-1). Therefore, a 3 dB must be subtracted from the abcissa values of these curves to account for the factor of 2 in this definition.

where the subscript i represents the ith sector. Performing this normalization
results in Table V-A. Note that these results assume that constant probability
of detection is desired for all sectors, which may not be the case. They can be
used, however, to derive a lower bound on the data interval obtained for a given
transmit power and probability of detection chosen from Figure 7.

Table V-A. Dwell Time Requirements Normalized to Sector 2.

Sector	T_i/T_2
1	1.683
2	1.0
3	1.683
4	.123
5	.077
6	.123
7	.011
8	.007
9	.011
	4.718

The data interval, or time between looks in a particular direction,
while covering the entire major sector coverage is essentially the total time
required to interrogate all sectors, Td. This can be bounded by the absolute
minimum, Td min, determined by

$$T_{d_{min}} = T_2 \sum_{i=1}^{9} \frac{T_i}{T_2} \qquad \text{(V-3)}$$

From Table V-A,

$$T_{d_{min}} = 4.718 \, T_2 \qquad \text{(V-4)}$$

Since Figure 7 is based on the basic single dwell interval of 20 milliseconds,
$T_2 = .02N$; therefore, the curves shown in Figure 8 can be drawn. These indicate
the transmitter power levels required for a given data interval for this radar
configuration. In effect, the transmitter power shown is continuous wave,
although it may be sequentially supplied by multiple units.

Figure 8 and Table V-A over-simplify the time-power resource allocation
considerably. A practical design would probably not normalize each minor
sector's dwell as shown in Table V-A. Instead, a suit of waveforms would be
chosen and applied by sectors, by function, and by desired detection criteria.
The considerations here serve only to illustrate the trade offs and the degree
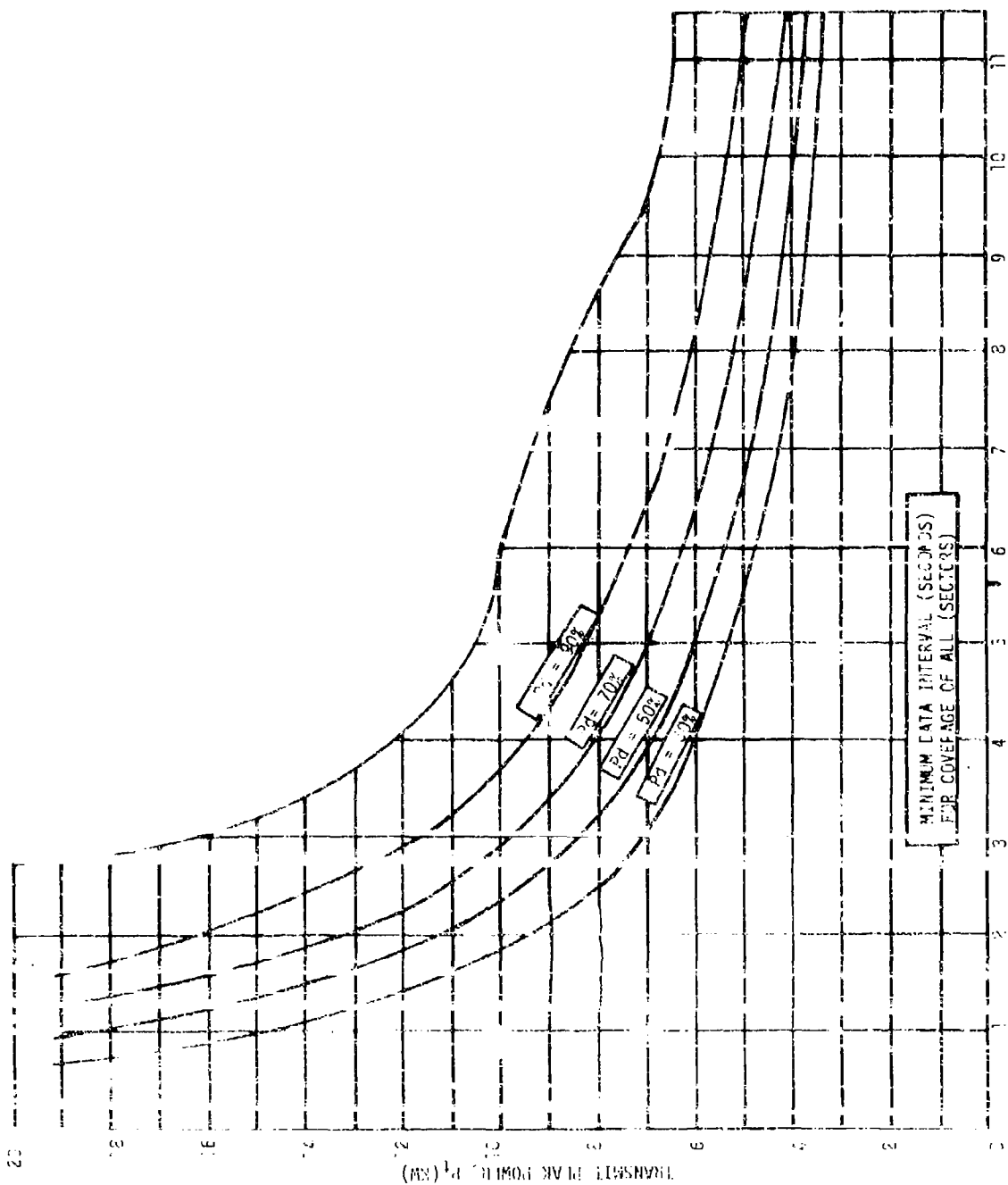of flexibility available.

Figure 3. Transmit power versus lower bound on data interval for interrogation of all the sectors at the probability of detection, P_d, value shown

Note that the coded wave forms suggested in the next section further support this philosophy of flexibility, since the desired performance parameters of resolution, ambiguity diagrams, instrumented range, and doppler extent are determined by the code choice, and are more or less independent of the time-power considerations.

VI. Waveform Design

A. Bi-Phase Coded Long Pulse

Extensive trade-off studies to compare various implementations of waveforms have not been done for the radar proposed here. There is rationale to support the choice of bi-phase coded long pulse (near CW) waveforms, and the examples that follow have counterparts with similar ambiguity and spectral characteristics in pulse doppler and frequency modulated waveforms. Therefore, the waveforms chosen are illustrative only.

The phase coded long pulses are relatively low peak power with near unity duty cycles. This is more compatible with solid state microwave power generation than the high peak power, low duty cycle pulse waveforms of traditional radar. The signature of these signals has fewer discriminants for the ARM receiver to sort by. There is no well defined leading edge to a number of pulses in a train; therefore, the ARM cannot leading edge gate to sort the direct path from a clutter bounce or a multi-path signal. The coded waveforms are extremely flexible; e.g., the ambiguity diagram is changed by code bit rates and code lengths. This can be done with software and digital circuit architecture rather than more significant hardware changes such as switched pulse compression lines or frequency synthesizer alteration, etc.

B. Bi-Phase Code Characteristics

A bi-phase, pseudo-random, maximum length code[4] is impressed on the microwave carrier by alteration of its phase between two states which are separated by 180 degrees. This alteration is done in a noise-like sequence at the code frequency (or bit rate), f_c, which establishes the bandwidth and the basic resolution of the coded waveform. These codes are deterministic, being easily generated by feedback shift registers. The bit length, τ, is

$$\tau = \frac{1}{f_c} \qquad (VI-1)$$

The number of bits, L, is constrained by the generation process to

$$L = 2^m - 1 \qquad (VI-2)$$

where m is the number of states in the shift register.

When applied as a waveform modulation for radar, the range cell size, ΔR, resulting from the code is given by

$$\Delta R = \frac{\tau c}{2} \qquad (VI-3)$$

where is the microwave propagation velocity. The unambiguous range, R_u is determined by the length of the code, t_s

$$t_s = L\tau \qquad\qquad (VI-4)$$

$$R_u = \frac{t_s c}{2} \qquad\qquad (VI-5)$$

The spectrum of the coded waveform has lines that are separated by f_c/L. If the target velocity has a radial component toward or away from the radar, a doppler shift of these spectral lines occurs either higher or lower respectively by

$$f_d = \frac{2V}{\lambda} \qquad\qquad (VI-6)$$

where f_d is the doppler frequency and v is the radial velocity.

If unambiguous doppler filtering is desired, the spectral lines must be separated by at least two times the maximum doppler frequency expected.* Thus, for unambiguous doppler filtering for a maximum radial target velocity of v_{max};

$$\frac{f_c}{L} = \frac{4V_{max}}{\lambda} \qquad\qquad (VI-7)$$

Substituting VI-7 into VI-5 with VI-1 yields

$$V_{max} = \frac{\lambda c}{8R_u} \qquad\qquad (VI-8)$$

where v_{max} is the maximum target velocity without ambiguities in the doppler filter space. Equation (VI-8) is plotted in Figure 9 showing the usual trade-off between range and velocity ambiguity.
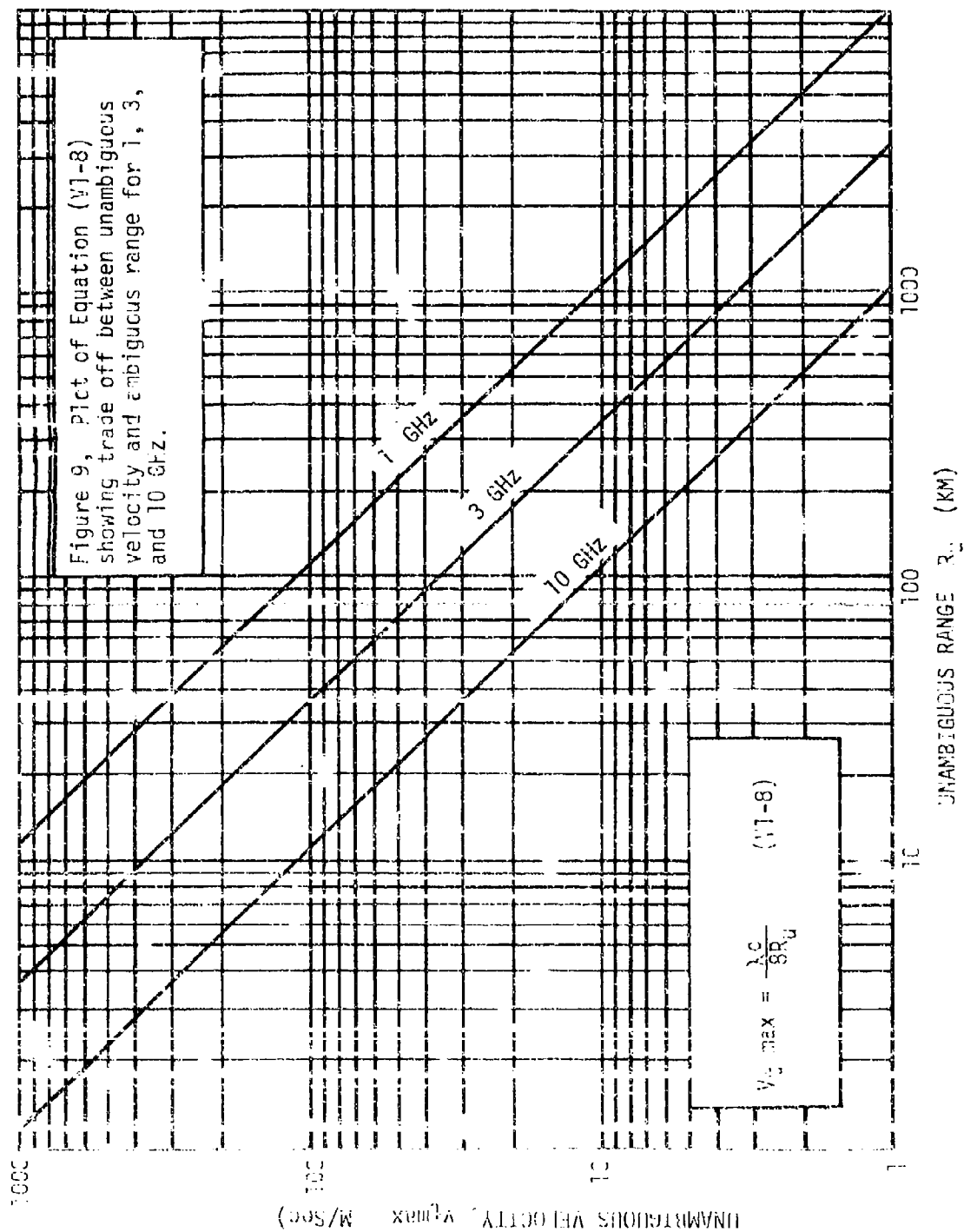
C. Range Cell Size Constraints

For long coherent integration times, the minimum range cell size is limited by the time required for the target to "fly through" the doppler filter used for

---

*Footnote: This is true if both approaching and receding targets are to be determined unambiguously. If a technique is used to first determine the target radial direction (by a range track file from previous looks, for example) the doppler filter space could be arranged so that the maximum doppler frequency could equal the spectral line separation before the ambiguity occurs. For this case, Equation (VI-7) becomes

$$\frac{f_c}{L} = \frac{2V_{max}}{\lambda} \qquad\qquad (VI-7a)$$

and Equation (VI-8) is

$$V_{max} = \frac{\lambda c}{4R_u} \qquad\qquad (VI-8a)$$

24

Figure 9, Plot of Equation (VI-8) showing trade off between unambiguous velocity and ambiguous range for 1, 3, and 10 GHz.

1 GHz

3 GHz

10 GHz

$$V_a\,max = \frac{\lambda c}{8R_u} \qquad (VI\text{-}8)$$

UNAMBIGUOUS RANGE R_u (KM)

UNAMBIGUOUS VELOCITY, $V_{a\,max}$ (M/sec)

coherent integration. The range cell, ΔR, necessary to cover this is

$$\Delta R = V_t\, t_f \qquad\qquad (VI-9)$$

Barton has suggested [5] that the range cell should be greater than this by at least a factor of 1.4 to reduce the range cell straddling loss, giving

$$\Delta R > 1.4\, V_{tmax} t_f \qquad\qquad (VI-10)$$

Note that this results in a maximum range cell size that can be used with the minimum range coherent integration time, t_f, from a single doppler filter. The target acceleration effects limit this integration time as discussed in the derivation of equation (IV-7).

If Equation (IV-7) is combined with (VI-10), eliminating t_f, the minimum range cell that can be achieved for a given maximum target velocity, V_{tmax}, and acceleration, a_t, is

$$\Delta R > 1.4\, V_{tmax}\sqrt{\frac{\lambda}{4 a_t}} \qquad\qquad (VI-11)$$

This is plotted in Figure 10, showing results for L, S, and X band radars with a range of 4 to 6 g targets. The code rate (or spectral bandwidth) of the waveform resulting from the minimum range cell is also plotted.

The radar designer would not use the minimum range cell given by equation (IV-10) unless the requirements called for very good resolution for target signature identification or perhaps extremely good distributed clutter performance. If used, the processor would be very complex because of (a) the code rates are high, (b) the number of range cells to be processed is high, and (c) the noncoherent integration string, necessary to cross a detection threshold, would have to include an ensemble of range cells, each covering a set of doppler cells.
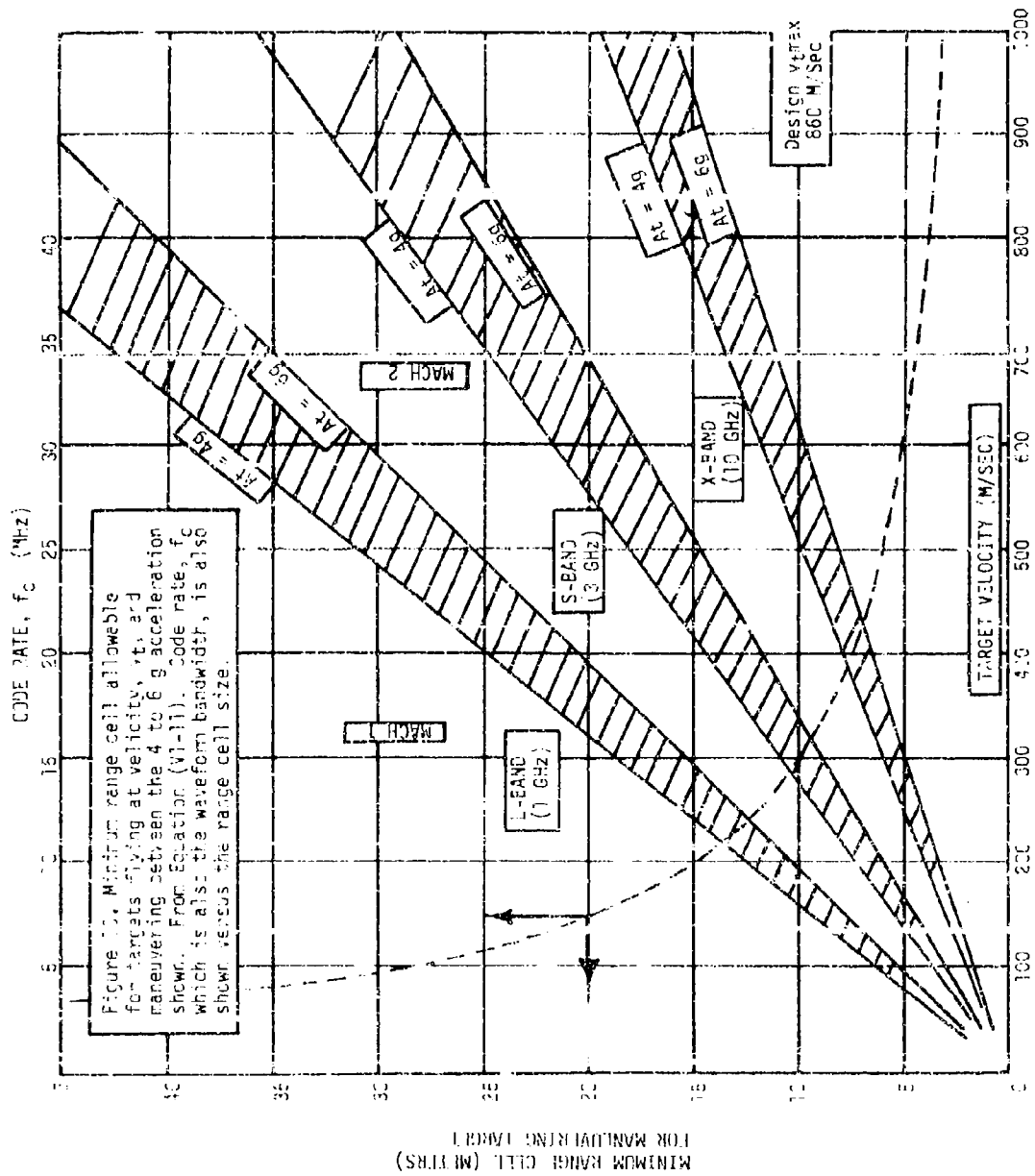
In order to prevent noncoherent integration over a large number of range cells the criteria is selected

$$\Delta R > 1.4\, V_{tmax}\, N t_f \qquad\qquad (VI-12)$$

where N is the number of coherent integration periods that are integrated non-coherently. (This N is the parameter used in Figure 7.)

D. Integration Process

The integration technique already discussed uses (a) the longest possible coherent integration interval, t_f, commensurate with the maneuvering target's changing velocity, and (b) a total dwell period, resulting from a

26

Figure 12. Minimum range cell allowable for targets flying at velocity, v_t, and maneuvering between the 4 to 6 g acceleration shown. From Equation (VI-11), Code rate, f_c, which is also the waveform bandwidth, is also shown versus the range cell size.

multiple, N, of these intervals

$$t_0 = Nt_f \qquad\qquad (VI-15)$$

which are integrated noncoherently. The total dwell period is determined by the average power requirements as discussed in Section V. The order of processing the information received at the antenna of a conventional radar is first, spatial direction (beam forming); second, range gating; and third, doppler filtering. For this type of radar, it is possible to alter this order since the beam forming as well as the range gating and doppler filtering are done in the digital processor. The reader will probably think through the integration string discussion that follows in the conventional order; however, one should keep in mind the possibility of integration strings in different orders. For example, where doppler processing is done first, giving priority to high velocity threat targets at close range, sorting out direction last.

In any case, the integration process requires the noncoherent addition of N outputs from the beam-range-doppler matrix. If the target were stationary (at constant direction, range, and velocity) then N sequential outputs from a single combination of beam, range, and doppler would be added for the target detection criterion. With a maneuvering target, however, the addition must follow the beam-range-doppler path of the target as it moves through the matrix. This sequence creates an integration "string." If the path of the string is not predictable, as is generally the case, all combinations of possible strings must be considered. The extent of these strings is bounded by the maneuvering target characteristics as discussed in the derivation of Equations IV-7, VI-10, 11, and 12.

Integration strings through a multi-dimensional matrix are fraught with difficulties. Note that the number of coherent intervals, N, adds another dimension to the matrix, namely time. In other words, it is not enough to determine a path in beam, range cell, and doppler space through the matrix; in addition, each of the N sequential intervals must be timed in its appropriate location.

An integration string concept could conceivably be replaced with an integration pyramid approach, where more cells than necessary were added to cover the growth in uncertainty of the target path as it moves through the matrix. These additional cells then, would add noise without signal and a collapsing loss would be encountered.

The perils outlined above suggest that it is better, by far, to reduce the number of dimensions of the matrix; e.g., to make sure that the cells of beamwidth, range, and doppler are large enough to encompass the target maneuver. If the coherent dwell interval is as long as possible for detection purposes per Equation (IV-7), the doppler cell dimension will not be large enough to encompass the more severe target maneuvers over more than one interval of t_f. Therefore, for Nt_f, one can certainly expect that an integration string will be necessary in the doppler dimension. If the radar resolution specifications are too strenuous, the beamwidth and range cells may also require strings. If this is the case, higher power transmitters, or smaller coverage sectors may be necessary to reduce the integration time and string complexity. It may also be feasible to relax the resolution specifications at

the longer ranges and implement them only at shorter ranges where less integration time is required.

In order to assess the severity of the integration string problem, the number of cells traversed by a target at velocity, V_t, and accelerating at a_t is determined below.

The number of beams, n_θ, traversed is given by

$$n_\theta = \frac{V_t \sin\gamma t_0}{\theta_a R} \tag{VI-14}$$

where θ_a is the 3 dB antenna beamwidth, R is the target range, and γ is the angle of the target's velocity vector with respect to the radial center line of the beam. Note that the $\sin\gamma$ term indicates that the target must have a crossing component to its velocity vector to traverse a beam. If $\gamma = 0$, the velocity is radial and $n_\theta = 0$, indicating a stationary target in the beam dimension of the detection matrix.

From Equation VI-14, it is obvious that at short range the number of beams traversed will be more than one. Of interest is the range at which this occurs; e.g., the minimum range at which only one range cell is required for all integration of the target returns. This is given by

$$R = \frac{V_t \sin\gamma t_0}{\theta_a}, \text{ for } n_\theta = 1 \tag{VI-15}$$

The number of range gates, n_r, traversed during the total integration period is

$$n_r = \frac{V_t \cos\gamma t_0}{\Delta R} \tag{VI-16}$$

where ΔR here is the range gate bounded by the absolute minimum range cell of Equation VI-10, or the more appropriate minimum of Equation VI-12 if permitted by more relaxed resolution requirements. The $\cos\gamma$ term indicates that the target velocity vector must have a radial component to traverse the range dimension of the detection matrix.

The number of Doppler filters, n_f, traversed is

$$n_f = \frac{2a_t \cos\gamma t_0}{\lambda B_f} \tag{VI-17}$$

Recall that the doppler filter bandwidth, $B_f = 1/t_f$. This and Equation (VI-15) substituted into the above yields

$$n_f = \frac{2a_t \cos\gamma M t_f^2}{\lambda} \tag{VI-18}$$

This form of the equation when n_f is proportioned to Nt^2_f indicates that for a given dwell time, t_0, there is an integration string advantage; e.g., n_f is smaller; if the dwell time can be achieved by using more noncoherent integration (larger N) and smaller coherent integration time, t_f. This is not advantageous for the detection process, however.

In order to maintain the entire noncoherent integration over a single doppler filter throughout the target maneuver for the total detection interval $t_0 = Nt_f$, then $n_f = 1$ and

$$t_f \leq \sqrt{\frac{\lambda}{2Na_t}} \qquad (VI-19)$$

assuming $\cos\gamma = 1$. Note that the above is similar to Equation IV-7 in form, but the denominator discrepancy between the two equations comes from the criteria. The above assures that the target will not out-maneuver a single doppler filter over the entire post detection integration interval, t_0, while Equation IV-7 attempts to assure that the target will not maneuver out of a single doppler filter during the coherent integration, t_f.

E. Code Selection

Codes will be determined here in order to illustrate the use of the criteria described in the previous sections. Figure 11 indicates some of the parameter relationships to clarify this process. Table VI-A lists the major descriptors of the code, their derivation source, and the resulting values.

Codes A and A' use a coherent interval, t_f, of 20 milliseconds. The total detection interval includes 30 of these (N=30) which are integrated non-coherently. From Figure 7, the power required is about 8.6 KW for 50% Pd. (A very low power for this class of radar.) However, a closer look at the integration strings required indicates a severe processing problem. Table VI-A shows that for code A, which is unambiguous in range to 250 km, the integration must be performed over 16.8 range cells ($n_r = 16.8$) and 14.1 doppler cells ($n_f = 14.1$). Code A', which is unambiguous in doppler for the 860 m/second target, must be integrated over 14.1 doppler cells also, although all of the integration could occur in one range cell ($n_r = .15$).

Codes B and B' illustrate waveforms which simplify the integration processing, but require more transmitter power. They use N=20 coherent intervals of $t_f = .005$ seconds each for a total integration period, t_0, of 0.1 seconds. This shorter integration time would require more transmitter power than codes A and A' in order to maintain the detection range. (The transmitter power would need to be increased to roughly 47 KW). Note that for B, the code with unambiguous range, and for B', for unambiguous velocity, the number of range cells per integration string, n_r, and the number of doppler cells per integration string, n_f, are always less than unity; therefore, the maneuvering target would not have to be chased through the range doppler matrix.

The above waveforms and codes serve only to illustrate the integration string considerations. Selection of a code must also consider blind speed elimination and the usual ambiguity plane problems. This radar design, with couple criteria on measuring the doppler history per se, may be near the limits imposed by these consideration chasing problems. Guidance
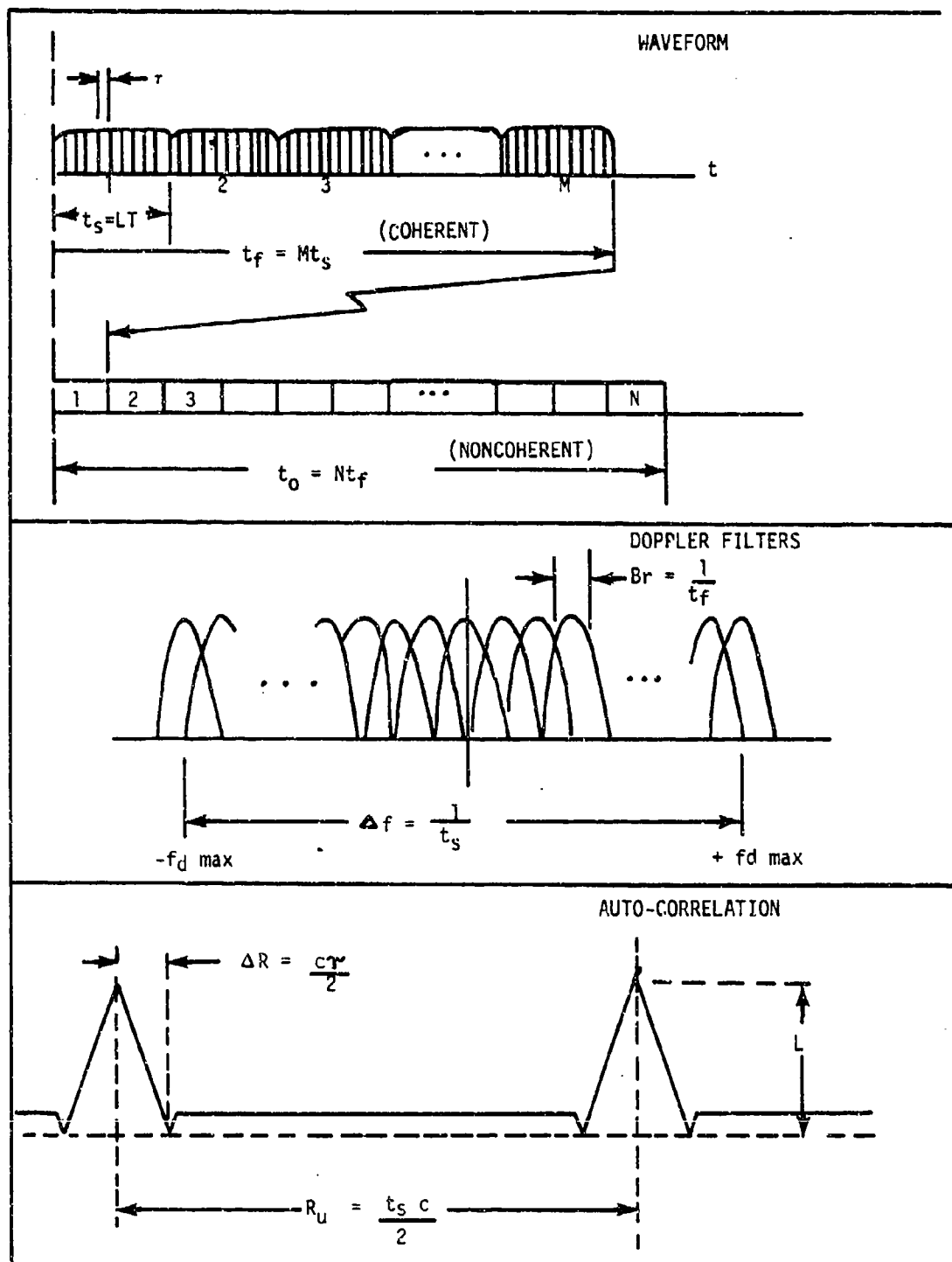
Figure 11.   Parameter and waveform relationship

31

TABLE VI-A. Major Descriptors, Derivation Source, and Resulting Values

PARAMETER	REF	EQUATION	UNIT	A	A'	B	B'	
MAX COHERENT INTEGRATION TIME, t_f MAX	IV-7	t_f max $\leq \sqrt{\dfrac{\lambda}{4a_t}}$	sec	.02	.02	*.005	.005	
MIN. DOPPLER FILTER WIDTH, B_f MIN		B_f min $= \dfrac{1}{t_f\,min}$	Hz	50	50	200	200	Parameters assumed for these calculations:
NUMBER OF NON-COHERENT INTEGRATIONS, N	IV-8	Fig. 7	--	30	30	20	20	$a_t = 6g = 58.8$ m/sec²
TOTAL DWELL TIME, t_o	VI-13	$t_o = N t_f$	sec.	.6	.6	.1	.1	$\lambda = 0.1$m
MIN. RANGE CELL SIZE, $\angle R$ MIN	VI-10	ΔR min $\geq 1.4\,V_t t_f$	M	24.1	24.1	6.02	6.02	$V_t = 860$ m/sec
MIN. RANGE CELL SIZE FOR NO STRING INTG'R	VI-12 VI-13	ΔR min @ $n_r=1$ > $V_t t_o$	M	722.4	722.4	86.0	86.0	$R_u = 250$ m desired
MIN. CODE BIT LENGTH, τ MIN.	VI-3	τ min $= \dfrac{2\Delta Rmin}{c}$	μsec	.1605	.1605	.573	.573	$c = 3 \times 10^8$ m/sec
TIME OF ONE CODE WORD, t_s FOR UNAMB. RANGE	VI-5	$t_s = \dfrac{2 R_u}{c}$	sec	.00167	-	.00167	-	$\theta_a = 2$ deg. = .035 rad.
TIME OF ONE CODE WORD, t_s FOR UNAMB. VELOCITY	VI-5 VI-8	$t_s = \dfrac{\lambda}{4 V\,max}$	μsec	-	29.07	-	29.07	Figure 16.
NUMBER OF CODE BITS IN ONE WORD, L	VI-2	$L \leq \dfrac{t_s}{\tau}\quad L = 2m - 1$	-	8191	127	2047	31	
BIT LENGTH CHOSEN, τ	VI-4	$\tau = \dfrac{t_s}{L}$	μsec	.204	22.89	.816	.938	
CODE RATE, OR SIGNAL BANDWIDTH, f_c	VI-1	$f_c = \dfrac{1}{\tau}$	kHz	4904.8	4368.8	1225	1065	
RANGE CELL CHOSEN, ΔR	VI-3	$\Delta R = \dfrac{\tau c}{2}$	M	30.6	3433.5	122.4	140.7	*Rather than the maximum coherent integration time, t_f max, this value of t_f was chosen on the basis of no integration strings, e.g., n_r <1 an n_f <1.
UNAMBIGUOUS RANGE, R_u	VI-5	$R_u = \dfrac{t_s c}{2}$		250.5	4.36	250.5	4.36	
UNAMBIGUOUS VELOCITY, V_u	VI-5 VI-8	$V_u = \dfrac{\lambda}{4 t_s}$	$\dfrac{M}{sec}$	14.97	860	14.97	860	
NUMBER RANGE CELLS PER INTEGR STRING, N_r	VI-16 VI-13	$N_r = \dfrac{V_t t_f}{\Delta R}$	--	16.86	.15	.703	.61	
NUMBER DOPPLER CELLS PER INTEGR STRING, n_f	VI-17 VI-13	$n_f = \dfrac{2a_t N t_f^2}{\lambda}$	--	14.11	14.1	.588	.588	
MIN. RANGE FOR SINGLE BEAM INTEGR', Rmin @ $n_\theta=1$	VI-15	R min @ $n_\theta=1$ = $\dfrac{V_t N t_f}{\theta_a}$	KM	14.8	14.8	2.46	2.46	

32

reduction in transmitter power will force $n_r > 1$ and $n_f > 1$ and beyond these limits will require multiple cell integration and increase the complexity of the processor significantly.

VII. Performance In Jamming
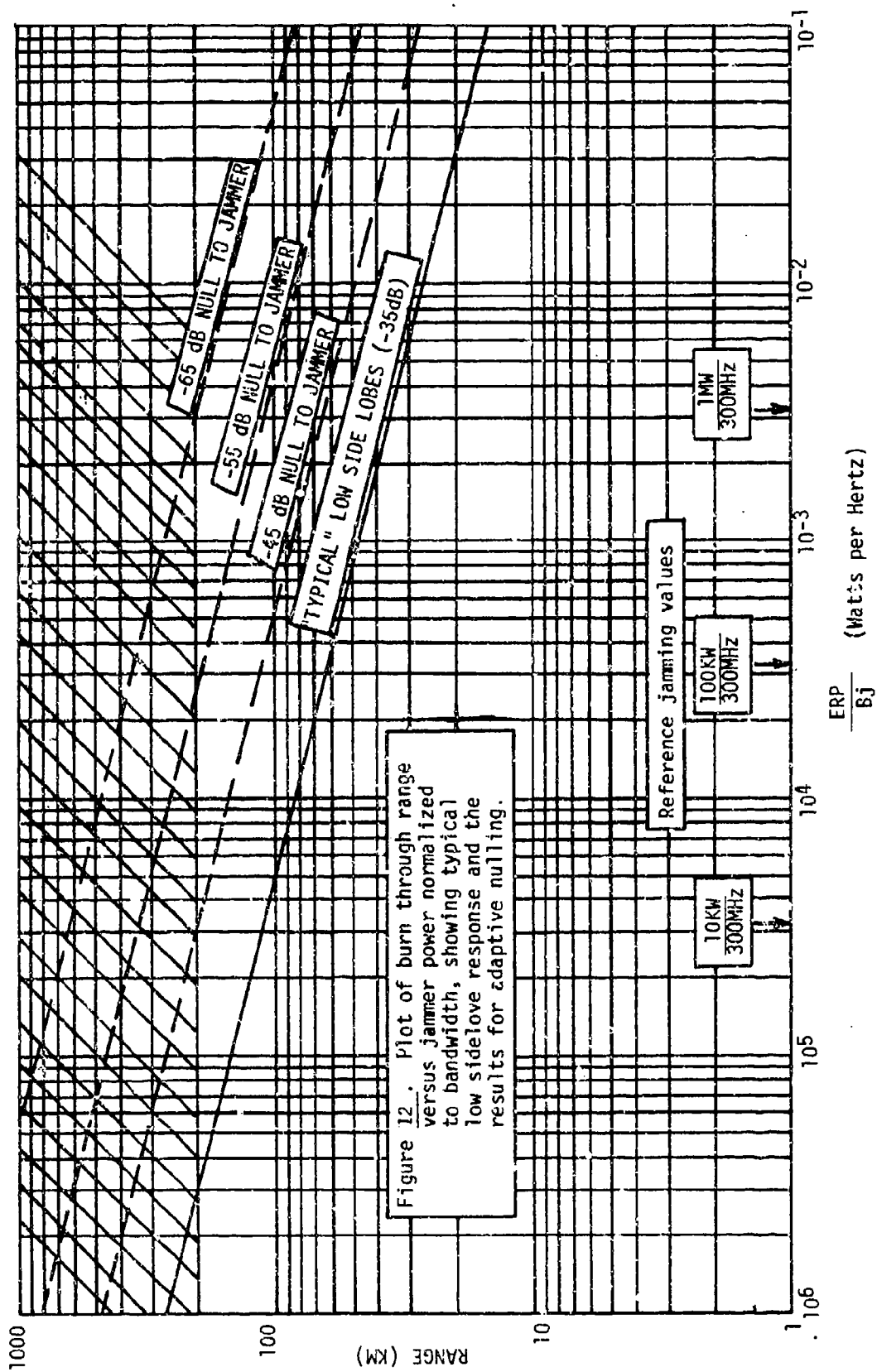
A. General Considerations

The current electronic countermeasure (ECM) threat for this class of radar is severe. Because of this modern radar design uses (a) pencil beam patterns to isolate the target return from a jammer outside the angular resolution of the main beam; (b) low sidelobes on receive in order to reduce the radar sensitivity to sidelobe jammers; and (c) frequency agility to force the jammer to spread its energy over a broad band, reducing its level of interference at the continuously changing frequency of operation.

The dispersed radar concept can use all of these standard techniques; however, their implementation needs examination. The pencil beam on receive is realized with the system suggested here. Each beam in the receive cluster is an independent pencil beam, and provides resolution for ECM.

In order to obtain very low sidelobes from the digital beamformer on receive, the errors in amplitude and phase at the receive module must be minimized. This is the same sort of problem encountered in conventional phased array antenna design. For example, in order to realize peak sidelobes in the range of 35 dB down from the main beam, random phase and amplitude errors over the entire ensemble of modular receive elements must be on the order of 15 degrees rms and 0.5 dB rms, respectively. Systematic errors across the major dimensions of the receive array must be even lower than these. Error specifications which are this low will present a challenge to the module designers and manufacturers, but they are achievable.

The digitally formed beams provide another possible ECM fix that is similar in concept to current techniques used in sidelobe cancelling. This is possible because the flexibility of beam forming by computer allows adaptive nulling. With the use of appropriate algorithms in the beamforming processor, nulls can be formed in the sidelobes on a beam by beam basis. This is done as a response to each of the directions from which jamming is received. The effect of this adaptive nulling is discussed in the derivation of Figure 12 .

It should be pointed out that it is conceptually possible to depress the adaptive nulls far beyond the error limited sidelobe levels. This may appear to be unrealistic because the same receive modules (with their errors) are involved in both the normal pattern formation and the adaptive nulling. However, the nulling algorithms, in effect, select the digital weighting coefficients for each element by using a closed loop process that compensates for the element errors; whereas the digitally formed beam before adaption uses an open loop algorithm that must set coefficients based on a' priori knowledge of the absolute errors at each element. If these errors were constant with frequency change, and over all temperature extremes, etc., the digital coefficients could be adjusted to "calibrate out" the errors, even for the open loop beam formation. A one time calibration is not expected to be feasible because of the poor behavior of the errors, leading to the need for a closed loop error correction scheme. This is only expected to be possible, however, on a periodic basis because of the time required for the calibration.

33

Figure 12. Plot of burn through range versus jammer power normalized to bandwidth, showing typical low sidelobe response and the results for adaptive nulling.

34

The above discussion leads to the conclusion that adaptive nulling, a closed loop process, is very similar to error compensation, also a closed loop process. Either of these requires iteration and thus consumes significantly more time (or processor complexity) than the original open loop digital beam formation. The question is: Can any of this be done on a beam by beam basis for radar use? How far the radar designer can take these concepts is directly dependent on the progress of the very high speed integrated (VHSIC) technology. This, of course, paces the implementation of real time processors for digitally formed spatial beams applied to radar.

Finally, the third ECM fix, that of frequency agility, can be implemented with the distributed radar but with less ease than in a conventional monostatic radar. The concept here, with approximately 500 to 1000 meter separation of equipments, lies in a grey area concerning the derivation of coherence betwen the transmit and receive functions. The question being: Is it easier to provide a common exciter for both functions as in monostatic design, or must we use separate exciters? The latter achieves coherence by an absolute standard, such as an atomic clock, at each equipment site; whereas the common exciter would have to be transmitted between the sites. One suspects that some hybrid of these approaches, e.g., a crude standard at each site which is periodically calibrated by a transmitted link, may be the most cost effective approach for this system geometry.

B.   Performance Calculations

The burn through range for target detection in the presence of sidelobe jamming is given by Equation VII-1 for the cases of interest (where the receiver noise is not significant compared to the jamming interference). Note that the bistatic range product, $R_1 R_2$, has been collapsed into a monostatic range to the target, R_t, on the assumption that $R_1 \approx R_2$.

$$R^4{}_t = \frac{P_t G_t SLL\sigma R_j{}^2 T}{4\pi L_1 D_1 \left(\dfrac{ERP}{B_j}\right)} \tag{VII-1}$$

where

R_t =   range to target
P_t =   transmit power
G_t =   gain of transmit antenna
SLL   =   receive sidelobe level with respect to receive mainbeam
σ =   radar cross section of target
R_j =   range to jammer
T =   detection interval of receiver
L_1 =   system losses, excluding receive loss
D_1 =   signal to jam ratio required for detection
ERP   =   effective radiated power from jammer
B_j =   jammer bandwidth

From Table VII-1 we obtain:

$$40 \log R_t = 157.6 - 10 \log \left(\frac{ERP}{B_j}\right) \qquad (VII-2)$$

This is plotted in Figure 12 as the solid line showing the range to the target at burn through for a 35 dB receive sidelobe level. If adaptive nulling is employed, the range performance is improved to the broken line plots where the nulling is indicated in 10 dB steps. Reference jamming values are shown on the absissa of the plot, where it is assumed that frequency agility will force the jammer to spread his ERP over the bandwidth of the 300 MHz shown.

Table VII-1. Dispersed Radar Performance Computation
in Sidelobe Jamming

Parameter	Value	dB	
		+	-
P_t	10 KW	40	
G_t	18.3 dB	18.3	
SLL	35 dB	35	
σ	$3M^2$	4.8	
$(R_j)^2$	$(150 \text{ km})^2$	103.5	
T	.02		17
4π			11
L_1	3		3
D_1	13		13
		$\overline{201.6}$ -44 $\overline{157.6 \text{ dB}}$	$\overline{44}$

VIII. Implementation Consideration

A. Transmit Equipment

The unique features required of the transmitter of this concept are the antenna pattern formation and the use of remote, unmanned, dispersed equipments. The need for registration of each of the transmitter's antenna pointing directions with the receive antenna pointing is somewhat unique and will require further study of procedures and/or equipment to facilitate site location and antenna positioning with low errors. Transmit exciter control, synchronization, waveform, and frequency management must be provided to the remote sites.

Two approaches considered here are for the transmit antenna. The first employs an ensemble of nine horns as shown in Figure 13. Each of the horns is designed and oriented to illuminate one of the minor sectors of Figure 3. The horn apertures range from about 15 x 35 cm (6 x 14 inches) to 12 x 17 cm (5 x 7 inches). A one to nine port switching network is required to sequentially switch the power amplifier's microwave output from sector to sector in concert with the other transmitters and the receive beam cluster. This is a series path network where the basic switches could be either ferrite or PIN diode devices. The losses of this type network will be on the order of 2.0 to 2.5 dB and each active switching device must handle the full power of the transmitter.

The second transmit antenna approach uses a single electronically scanned antenna, a small planar array with phase control for each element. Its aperture is on the order of 15 x 35 cm (6 x 14 inches) with four element rows by 8 element columns, using a total of 32 elements. These are uniformly illuminated with a corporate waveguide feed. Therefore, each phase shifter handles 1/32 of the total transmit power output and there is only one active device (a phase shifter) in each path. Losses for this network should be on the order of 1.0 to 1.5 dB; therefore, it appears to be more promising than the switched horn approach.

The array should be tilted back from the vertical at the same angle (13.1°) as the receive array. Its natural beam spoiling with scan will assure a similar coverage sector as that of the receive array. However, the phase control permits further beam spoiling and tailoring to a particular sector coverage, if required. The fine alignment of pointing direction with the other units can be done electronically by adjusting two constants in the beam steering programmer; whereas, the switched horn approach would require both fine and coarse alignment to be done mechanically. Alignment of the transmit and receive arrays should be possible by transmitting a null (formed in azimuth, or elevation, by adding a 180° phase shift to one half of the array) then sweeping the receive cluster's center beam through it to determine the alignment error. The beam steering controller would not be much more complicated than the control of the switches of the horn feed network. For these reasons, the planar array appears to be the favored approach for the transmit antenna.
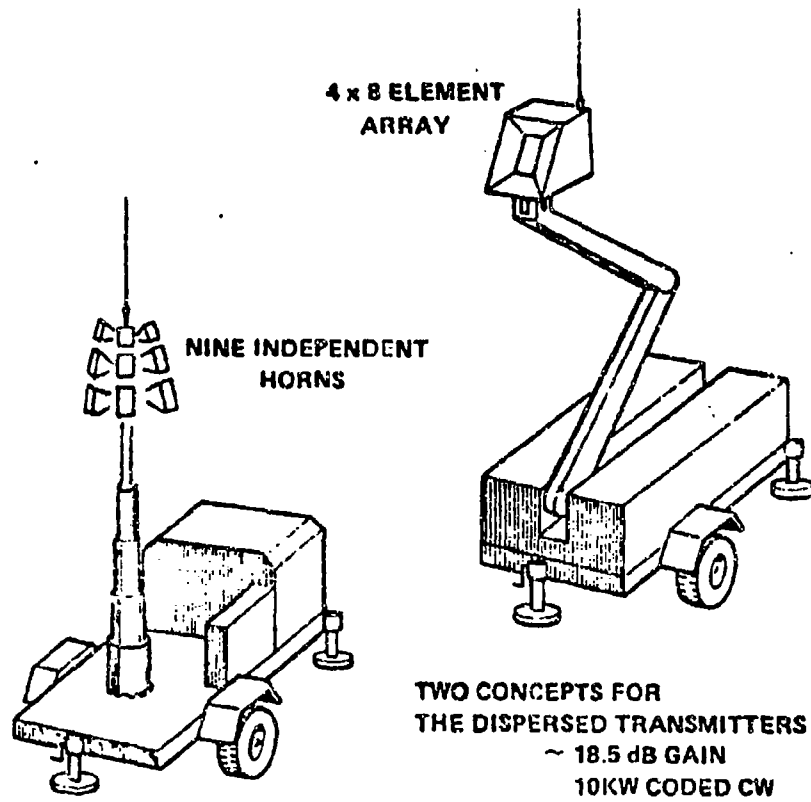
4 x 8 ELEMENT ARRAY

NINE INDEPENDENT HORNS

TWO CONCEPTS FOR THE DISPERSED TRANSMITTERS
~ 18.5 dB GAIN
10KW CODED CW

Figure 13. Transmitter configuration concepts.

B. Receive Unit

The receive site is manned and is located with or near the air defense command post. The antenna, processor, and data reduction requirements are technically challenging due to the use of 200 simultaneous receive beams and the need for real time data retrieval. In addition, the jamming threat environment requires that the sidelobes for each of the receive beams be as low as feasible. This means that extremely low phase and amplitude error budgets must be placed on the antenna components and receive modules.

The receive site equipment, shown conceptually in Figure 14, consists of a receive-only, solid state planar array; a beam forming digital signal processor; central control and data links to the remote transmitters; data links to the air defense net; and operator space. The basic antenna aperture required for a 2 degree pencil beam using a circular Taylor illumination function [2],n=8, has a diameter of 38 wavelengths at 3.0 GHz, this represents an array diameter of 3.8 meters (12.5 ft). Figure 15 indicates an equilateral triangle array lattice which efficiently spaces the elements to scan over a 60 degree cone from broadside. The elemental area of this lattice, shown as .289λ^2, divided into the array area yields the number of elements required, 3924.

At each element of the array there is a solid state modular receiver which coherently down converts from the S-band microwave target returns to baseband. Each module has sample and hold analog to digital (A/D) conversion at its output. These modules are all identical...note that there are differences from current solid state array concepts:

1. The array is receive only. Therefore, the usual incompatability of placing microwave power generation circuits on the same module as low noise receiver circuits is eliminated.

2. There are no phase shifters involved.

3. The outputs are not collected or summed in an RF or IF manifold. The outputs are digital words which interface directly with a digital processor.

The digital outputs of the in-phase and quadrature channels of the 3,924 elements of the array are independently routed directly to the input of the processor. This allows the processor to work in the spatial regime as well as the usual time and frequency regimes. The A/D conversion is done in elemental channels which have the gain of only one element. Therefore, the dynamic range of these A/D converters is reduced by a factor of 1/N over a conventional array of N elements where the summing is done before A/D conversion. This means that, to support the dynamic range requirement, 6 bit (or less) A/D's can be used. However, studies need to be completed concerning the A/D dynamic range that is needed for the very low error budgets necessary for ultra-low sidelobe receive patterns. Another area of concern is the sample and hold circuits that must preceed A/D conversion. These must include linear video amplification that is adequate enough to allow the receiver noise to toggle the A/D's smaller bits.
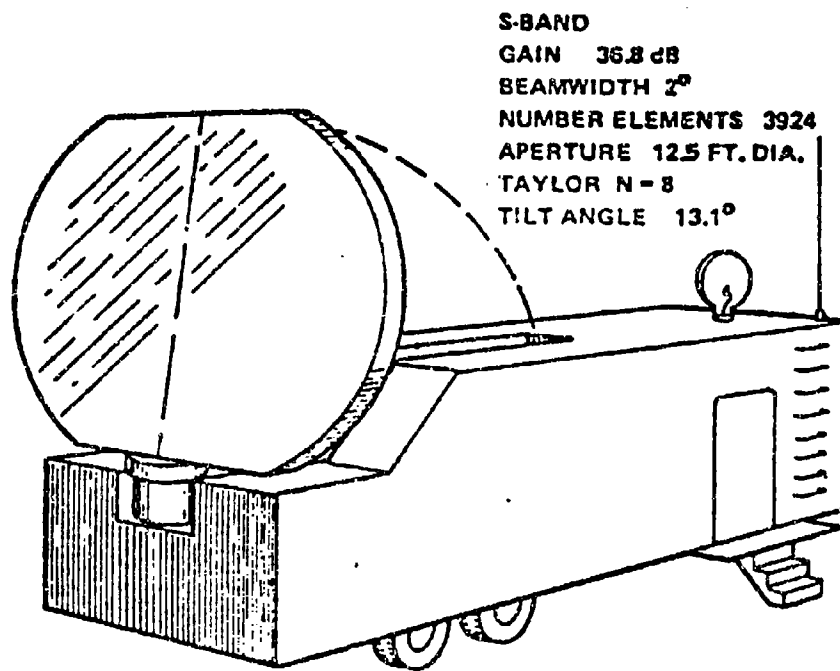
S-BAND
GAIN 36.8 dB
BEAMWIDTH 2°
NUMBER ELEMENTS 3924
APERTURE 12.5 FT. DIA.
TAYLOR N = 8
TILT ANGLE 13.1°

Figure 14. Receive site concept
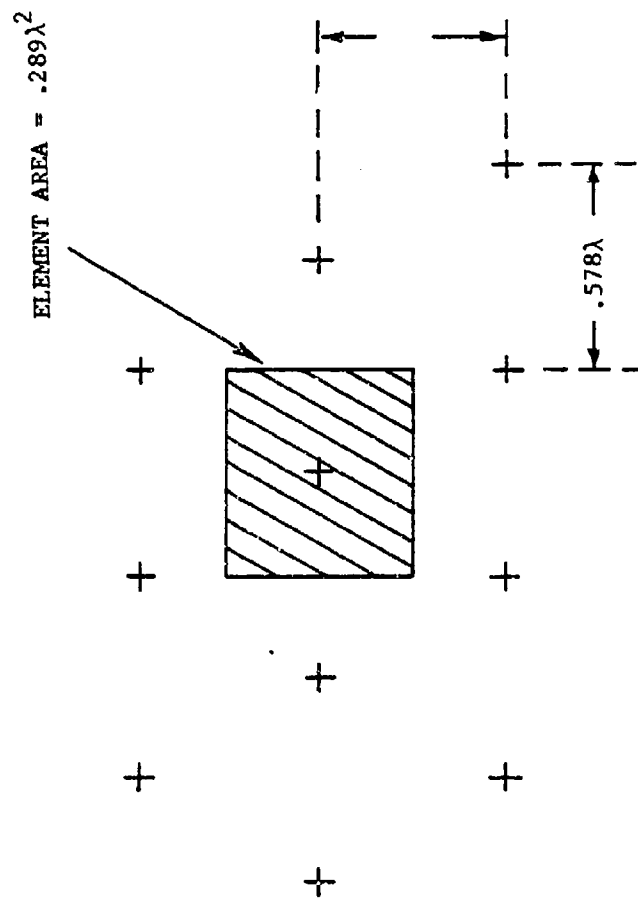
ELEMENT AREA = $.289\lambda^2$

$.578\lambda$

Figure 15. Element location lattice for receive planar array

41

A/D sample rate requirements are driven by the range cell size needed by the radar. In essence, this is given by

$$f_c = \frac{c}{2\overline{\Delta R_{min}}}$$

where f_c is the sample rate (or code rate) and ΔR_{min} is the minimum range cell used by the radar. Although many A/D circuits can now be obtained in an integrated circuit format, the above factors require a careful scrutiny. It may be necessary to develop the A/D in order to meet the unique requirements of a given radar design. Additional study is required in this area.

Beam forming can be done with either a two dimensional fast Fourier transform (FFT) or a discrete Fourier transform (DFT). The formation of simultaneous beams in space is done entirely within the digital processor, and is a natural consequence of using modern digital Fourier transform methods. However, decoding, parallel processing of range and doppler, resolving ambiguities, and performing constant false alarm rate (CFAR) management on 200 simultaneous beams does challenge the current digital processor art.

The US Department of Defense is currently engaged in a multi-year program to improve processing capability through a very high speed integrated circuit (VHSIC) technology development program. An FFT butterfly* circuit is promised in three years that will function in 40 nanoseconds using a circuit that is 1 cm^2 in area.

Using a very crude approach, one can at least determine an estimate for a bound on the beam forming time that would result if this butterfly chip were used:

1. A 64 x 64 element array input would result in 4,096 elements in the array, a number reasonably close to the 3,924 required above by the antenna pattern considerations.

2. A brute force two dimensional FFT approach for beam forming would simply use 64 columns of FFT's having 64-point inputs each. Their outputs would feed 64 rows of another set of 64-point FFT's. The output of this matrix would yield 4,096 beams. These beams are not positioned in space properly in order to select from among them the specific 200 beams required here. However, the time required to perform the operation to produce the 4,096 beams may serve to get a feel for the emerging art.

3. A 64-point, radix 2, FFT has 6 tiers or "sequential layers" of butterfly operations that must be done in sequence.

4. If we assume that all column FFT devices are redundant and operate in parallel and that the same is true for the rows, then for time computation purposes, two groups of 64-point FFT's must operate in sequence.

---

* The butterfly is the basic circuit required in an FFT. It performs one complex multiplication and two complex adds.

5. Therefore,

> For the 6 tiers of buterflys in sequence:
> 6 x 40 nanoseconds = 240 nanoseconds
> (e.g., a 64-point FFT requires 240 nanoseconds).
>
> For the two groups of FFT's done sequentially:
> 2 x 240 = 480 nanoseconds

6. This crude estimate would support a sample rate of $1/(480 \times 10^{-9}) = 2.08$ MHz.

The above sample rate ultimately defines the signal bandwidth that is achievable for the radar waveform. The range cell size resulting from this 2.08 MHz bandwidth is determined from Equation VIII-1 as 72.1 meters. It is clear that this is a useable range cell size for this radar application. The above example assumes the entire beam former clears for each sample set. A pipe line processor could reduce this time considerably by delaying the output by a few sample intervals.

This crude example indicates that the processor technology will support digital beam forming in the near future. To realize its full potential for an air defense radar, algorithms and processor architecture need to be developed which will allow real time adaptive nulling and pattern tailoring to an ECM environment.

IX. Conclusions

A radar concept has been discussed which offers a potential solution to the major problems facing the air defense radar community in the next decade. These solutions are not thoroughly addressed in this first concept paper; however, they can be indicated here as justification for further development of the concept.

(1) Antiradiation missiles -

Good immunity is inherent by the dispersed nature of the transmit function and the totally passive receive site.

(2) Standoff jammers -

The use of digital beam forming allows adaptable spatial filtering, e.g., the ability to place antenna pattern nulls in the directions of the jammers, both in the sidelobes and on the skirts of the main beam.

(3) Escort jammers -

The dispersed equipment provides the geometry to perform noise correlation for determining the range of escort jammers. Although not discussed herein, a modest receive function added to the dispersed transmitters would enable rough triangulation at the normal receive site.

Implementation of this concept requires advanced technology. Very high speed integrated circuits (VHSIC) are required for processing the information from multiple beams in range, doppler, and angular space. The latter, digital processing in angular space, is a new and emerging technology[6] with considerable hardware and algorithm development needed for radar application, although it is a more mature art for slower sample rate applications of sonar and geophysics applications.

Solid state array technology is employed. The receive only module uses coherent microwave integrated circuits which are within the current art. Each module also includes video circuits and analog to digital conversion which is "available," but will require development effort to be reasonably compatible with the array module application.

This concept uses a multi-static radar geometry. A conclusion is implicit in this report, however, that the equipment should not be widely dispersed. Therefore, a sanctuary is not provided for the transmitter; instead, ARM immunity is gained by dispersing the transmit function over a region relatively close to the receive site.

The concept described is futuristic but well founded in the near-term trends and technology development required to support it. It is therefore important, because it illustrates to the military user the performance advantages to be gained through development and exploitation of a new level of technology base – solutions to problems for which there are very few satisfactory answers in the existing radar concepts using the existing technology base.

X. RECOMMENDATIONS

In order to exploit the techniques suggested here, additional work is needed in the following areas:

A. Parallel Beam System Concepts

Current radar design uses a sequentially scanned beam which is sequentially processed for each direction in space. System concepts are allowed by the techniques herein which use multiple simultaneous beams. If the radar must provide very high data rates in a target rich environment, or if the dwell time must be extremely long for high doppler resolution processing, then these parallel beam approaches should be considered. Concept studies are needed to optimize the number of beams, waveforms, etc. for a given application.

B. Dispersed Transmitter Studies.

Dispersed transmitters are suggested here as a means to handle the ARM's in a manner similiar to that of blinking decoys. More definitive study of this is needed to show trade-offs between the blinking scheme effectiveness and radar performance. Use of the dispersed transmit farm can also be studied for other purposes, such as for target fluctuation improvement, or triangulation for range information on escort jammers.

44

C. Tracking and Beam Splitting Studies.

Tracking techniques for this class of system need to be addressed. The use of multiple beam clusters is similiar to the four beam cluster required for monopulse tracking; therefore, questions arise: Should the processor treat every adjacent set of beams as a tracking set with sum and difference processing available on every target detection or should a special set of tracking beams be employed for better accuracy? Is beam splitting necessary, or can a scanned sequential cluster set be used to pinpoint a target direction in space? With spatially sampled digital beam forming, can the tracking be done with spatial filtering using modern high resolution filtering techniques?

D. Digital Beamforming.

Both open loop and closed loop digitally formed spatial beams need study. In particular, algorithms for forming beams, compensating for manufacturing errors, and forming nulls to directional sources of interference (all in real time) need investigation. The impact of VHSIC on the beamforming capability needs more rigorous assessment. The use of new digital filtering techniques, such as the maximum entropy methods for enhanced resolution, should be investigated for this application.

E. Processor Architecture.

The digital signal processor required here must adaptively form multiple simultaneous beams and process all of their signals from a given sector of space within the dwell time allowed for that sector. This will require VHSIC implementation. Architecture studies are needed which provide processor designs centered around the chip set to be produced by the US Department of Defense VHSIC program.

F. Component Development.

This concept is based on the use of a receive module per element in a large planar array. Down conversion is needed that is coherent from module to module across the array face. Linear amplification is needed at a low IF or video to drive the sample and hold of a modular A/D converter (for both in-phase and quadrature channels) on the rear of each receive module. A program is needed to develop a family of these receive modules for digital beamforming applications such as the one described herein. This should include the development of low logic power circuits with appropriate form factors.

Appendix A

Receive Array Tilt Angle Determination

For most air defense coverage volumes the envelope of the peak gain of the pencil beam receive array, versus scan from broadside, is optimized over more of the scan volume if the plane of the array face is tilted back from vertical. One criteria to use for the determination of this tilt angle is simply to equalize the maximum scan angles from the array broadside that occur when the array is scanned to each of the extreme "corners" of the coverage volume. The scan angle from broadside, θ, given by Ref 2 is

$$\theta = \cos^{-1}\left(\sin E \, \sin T + \cos E \, \cos A \, \cos T\right) \qquad (A-1)$$

where E and A are the earth elevation and azimuth angular directions and T is the tilt back angle of the array face with respect to the zenith of the earth coordinates.

The coverage volume is symmetric about its azimuth center; therefore, the coordinates of $+60^\circ$ A , 0° E and $+ 60^\circ$ A , 50° E can be substituted into (A-1) yielding two simultaneous equations which are solved for T when the θ of each of these cases are equated. When this is done the tilt angle computed is 13.12° which was used in the determination of the sector boundaries of Figure 3. Note that the upper sectors extend to 62.4° rather than the 50° E used above. Further iteration of the tilt angle and sector boundaries was not done for this example, but in principle the tilt angle can be adjusted to enable reasonable extremes of the angle from broadside, θ, to be used for the coverage extremes.

REFERENCES

1. Peter J. Kahrilas, <u>Electronic Scanning Radar System Design Handbook</u>, ARTECH HOUSE, Inc., 1976.

2. J. V. DiFranco and W. L. Rubin, <u>Radar Detection</u>, Prentice-Hall, Inc., 1968.

3. D. K. Barton and H. R. Ward, <u>Handbook of Radar Measurement</u>, Prentice-Hall, Inc., 1969.

4. R. C. Dixon, <u>Spread Spectrum Systems</u>, John Wiley and Sons, 1976.

5. D. K. Barton, Private Communication.

6. W. G. Spaulding, "Array Signal Processing for Radar (An Introduction and Assessment for MIRADCOM Interests)", T-79-11, 5 February 1979.

DISTRIBUTION

ADDRESSEE	NO. CYS
DRSMI-LP, Mr. Voigt	1
-RPR	15
-RPT, Record Copy	1
-RER, Mr. Spaulding	50